Available online at www.sciencedirect.com
ScienceDirect
Journal of Sound and Vibration 317 (2008) 716–738
JOURNAL OF SOUND AND VIBRATION
www.elsevier.com/locate/jsvi

Dynamic analysis of space frames: The method of reverberation-ray matrix and the orthogonality of normal modes

Y.Q. Guo, W.Q. Chen*, Y.-H. Pao[1]

Key Laboratory of Soft Soils and Geoenvironmental Engineering, Ministry of Education, Department of Civil Engineering, Zhejiang University, Hangzhou 310027, PR China

Received 23 January 2008; received in revised form 25 March 2008; accepted 29 March 2008
Handling Editor: L.G. Tham
Available online 19 May 2008

Abstract

The formulation of reverberation-ray matrix analysis has been proposed to study wave propagation in planar frames. It is applied here to modal analysis of complex three-dimensional framed structures, optionally with lumped masses and/or elastic supports. Furthermore, by means of Betti's reciprocity theorem, orthogonal conditions are established for different natural modes, and hence transient response analysis based on mode superposition is developed. Both the reverberation-ray matrix analysis for free vibration and the mode superposition method for transient response are illustrated by numerical examples.

1. Introduction

Structural dynamics is an important theoretical basis of many engineering activities associated with engineering structures, such as design, construction, control, damage detection and seismic resistance. It generally consists of two functions, i.e. free vibration analysis (modal analysis) and response analysis (steady-state and transient analysis). Free vibration analysis is to find natural frequencies and natural modes, which are the intrinsic dynamic properties of a structure. Response analysis is essential for evaluating the mechanical behavior of structures since it gives relations between the intrinsic properties of structures and the external excitations. Consequently, it is very important to develop approaches for reliable and accurate dynamic analysis of structures [1].

Framed structures have been commonly used in civil and aeronautical engineering, such as long-span bridges, high-rise buildings, offshore platforms, aircrafts and space vehicles, to name a few. Many dynamic analysis methods for framed structures have been developed in matrix forms, which are suitable for computer programming. Well-known examples include finite element method (FEM) [1], exact dynamic stiffness method (EDSM) [2–4], transfer matrix method (TMM) [5], spectral element method (SEM) [6], and wave traveling

*Corresponding author. Tel.: +86 571 87952284; fax: +86 571 87952165.
E-mail address: chenwq@zju.edu.cn (W.Q. Chen).
[1]Professor Emeritus, National Taiwan University, China and Cornell University, USA.

0022-460X/$ - see front matter © 2008 Elsevier Ltd. All rights reserved.
doi:10.1016/j.jsv.2008.03.052

approach (WTA) [7,8]. The method of reverberation-ray matrix (MRRM) has been proposed based on a much different physical basis from all existing methods [9–14], as will be shown later.

FEM, since its birthday around 1960, has demonstrated the wonderful power in solving engineering problems. With FEM, natural frequencies and natural modes could be easily obtained by solving a generalized eigenproblem, and the mode superposition method, which is based on the orthogonality of natural modes, could be used as an alternative for transient response analysis [1,15–19]. However, finite element method is approximate rather than exact, although the accuracy of results generally could be improved by increasing the number of discrete elements. In particular, it will become computationally expensive for problems of wave propagation, high-frequency response due to impact load, etc.

In contrast to FEM, EDSM employs exact solutions of the governing equations of a structural member without any approximation. Since the corresponding characteristic equation, which determines the frequencies, is a transcendental equation, special algorithms should be developed [2,3,20–28]. TMM also starts from exact solutions, but formulated in a state space. It is very suitable for structures with units linked end to end to form a chain. Note that both EDSM and TMM contain hyperbolic sine and cosine functions in the resulting frequency equation. These functions with a positive index grow exponentially with the frequency or length of structural member. Thus, numerical instability may be encountered in the numerical calculation [5,13,29]. Nagem and Williams [30] proposed an interesting approach by combing the transfer matrix with the joint coupling matrix. Their approach can partly avoid the numerical difficulty in TMM by, in certain sense, reducing the length of transfer, but not completely.

On the other hand, the numerical instability can be completely removed in SEM, WTA and MRRM, all employing exact solutions also, but in a traveling wave form. Formulations that are stable for numerical calculation can be established by dividing waves in a member into two catalogues, i.e. arriving waves and departing waves. Therefore, as a supplement to the powerful FEM, these three or other similar methods should be appealing when high-frequency response is to be evaluated.

Here in this paper, we pay our attention to MRRM only, which is extended to modal analysis of three-dimensional (3D) frames with or without lumped masses and elastic supports. Preliminaries of elastodynamics of 3D frames are presented in Section 2. Formulations of MRRM for free vibration analysis are concisely summarized in Section 3. A special algorithm is proposed, by which the numerical difficulty in determining natural frequencies from complex-valued determinant as mentioned by Luongo and Romeo [31] is avoided successfully. In Section 4, starting from Betti's reciprocity theorem [32], the orthogonal conditions of different natural modes are established. The mode superposition method (MSM) is then formulated for the transient response analysis of structures. A remarkable feature of MSM is that distributed forces can be treated as well, while in the traditional MRRM only concentrated forces applied at joints can be considered. Numerical examples are given in Section 5 to validate the effectiveness of MRRM for free vibration analysis and the feasibility of MSM for transient response analysis of complex 3D framed structures. The paper ends with some conclusions drawn in Section 6.

2. Elastodynamics of 3D frames

2.1. Dynamic state of a space slender structural member

An arbitrary structural member in a 3D framed structure is seen as the carrier of longitudinal wave, torsional wave and flexural (transverse) waves in two principal planes of cross section. All three types of waves propagate independently in the member, but they are coupled by wave scattering at joints. Let the centroid of all cross sections be a straight line and coincide with the x-axis of the local Cartesian coordinate system (x, y, z). The motion of the member is described at each cross section perpendicular to the x-direction by six components of a generalized displacement vector $\boldsymbol{\delta} = [u, v, w, \varphi_x, \varphi_y, \varphi_z]^{\mathrm{T}}$, which exactly corresponds to a generalized force vector $\mathbf{f} = [N_x, Q_y, Q_z, M_x, M_y, M_z]^{\mathrm{T}}$ of six components. Combining together all components of the generalized displacement and force vectors gives the state vector $\mathbf{v} = [\boldsymbol{\delta}^{\mathrm{T}}, \mathbf{f}^{\mathrm{T}}]^{\mathrm{T}}$, which describes the dynamic state of the structural member at any cross section. It depends on the coordinate x and time t.

2.2. Governing equations

The classical longitudinal rod theory, the Timoshenko beam theory, and the elementary torsional shaft theory are adopted to describe the axial, flexural and torsional waves respectively. The corresponding governing equations are

$$\frac{\partial}{\partial x}\left[E(x)A(x)\frac{\partial u}{\partial x}\right]+q_x(x,t)=\rho(x)A(x)\frac{\partial^2 u}{\partial t^2} \tag{1}$$

for the axial wave,

$$\begin{aligned}&\frac{\partial}{\partial x}\left[\kappa_y G(x)A(x)\left(\frac{\partial v}{\partial x}-\varphi_z\right)\right]+q_y(x,t)=\rho(x)A(x)\frac{\partial^2 v}{\partial t^2}\\&\frac{\partial}{\partial x}\left[E(x)I_z(x)\frac{\partial \varphi_z}{\partial x}\right]+\kappa_y G(x)A(x)\left(\frac{\partial v}{\partial x}-\varphi_z\right)+m_z(x,t)=\rho(x)I_z(x)\frac{\partial^2 \varphi_z}{\partial t^2}\end{aligned} \tag{2}$$

for the flexural wave in *xoy* plane,

$$\begin{aligned}&\frac{\partial}{\partial x}\left[\kappa_z G(x)A(x)\left(\frac{\partial w}{\partial x}-\varphi_y\right)\right]+q_z(x,t)=\rho(x)A(x)\frac{\partial^2 w}{\partial t^2}\\&\frac{\partial}{\partial x}\left[E(x)I_y(x)\frac{\partial \varphi_y}{\partial x}\right]+\kappa_z G(x)A(x)\left(\frac{\partial w}{\partial x}-\varphi_y\right)+m_y(x,t)=\rho(x)I_y(x)\frac{\partial^2 \varphi_y}{\partial t^2}\end{aligned} \tag{3}$$

for the flexural wave in *xoz* plane, and

$$\frac{\partial}{\partial x}\left[G(x)I_x(x)\frac{\partial \varphi_x}{\partial x}\right]+m_x(x,t)=\rho(x)I_x(x)\frac{\partial^2 \varphi_x}{\partial t^2} \tag{4}$$

for the torsional wave. In the above equations, $u(x,\ t)$, $v(x,\ t)$ and $w(x,\ t)$ are components of translational displacement in x-, y- and z-directions, respectively; $\varphi_x(x,\ t)$, $\varphi_y(x,\ t)$ and $\varphi_z(x,\ t)$ are rotations of the cross section at position x about the x-, y- and z-axes, respectively; the cross sectional area A, its second moments about x-, y- and z-axes, I_x, I_y and I_z, mass density ρ, Young's modulus E, and shear modulus G can be functions of x as indicated. The shear coefficients κ_y and κ_z are introduced to take account of the shear deformation in the beam, both assumed to be constants. Eqs. (1)–(4) can be rewritten concisely in a matrix form as

$$\mathbf{L}\boldsymbol{\delta}(x,t)=\mathbf{M}\ddot{\boldsymbol{\delta}}(x,t)-\mathbf{q}(x,t) \tag{5}$$

where

$$\mathbf{M}=\rho(x)\mathrm{diag}\left[A(x),A(x),A(x),I_x(x),I_y(x),I_z(x)\right],\quad \mathbf{L}=\begin{bmatrix}\mathbf{L}_{11} & \mathbf{L}_{12}\\ \mathbf{L}_{21} & \mathbf{L}_{22}\end{bmatrix}$$

are operator matrices with respect to mass and stiffness properties, respectively, and $\mathbf{q}=[q_x,\ q_y,\ q_z,\ m_x,\ m_y,\ m_z]^{\mathrm{T}}$ is the external force vector. The elements of operator matrix $\mathbf{L}$ are given in Appendix A. The dot over a quantity denotes partial differentiation with respect to time. For a non-uniform member, although solution to Eq. (5) can be expressed in terms of the propagator [33], it is not easy to perform calculation for a practical problem. Alternatively, one can divide the member along the x-axis into many segments of small length. Each segment can be approximated by a uniform member with constant geometric and material parameters. In so doing, the number of members and that of joints increase, but the analysis procedure keeps unaltered. Hence, in MRRM, we will assume that all members in the structure are uniform. On the other hand, the orthogonality of natural modes can be established for a structure with non-uniform members, as to be shown in Section 4.

2.3. Solutions

As is well-known, the general solution of an inhomogeneous equation is the summation of a particular solution and the supplementary solution corresponding to the associated homogeneous equation. We first consider the homogeneous counterpart of Eq. (5). By the method of separation of variables, one assumes

$$\boldsymbol{\delta}(x,t) = \hat{\boldsymbol{\delta}}(x;\omega)r(t) \tag{6}$$

where all components of the generalized displacement vector vary in unison with time variable t. Substituting Eq. (6) into the homogeneous counterpart of Eq. (5) gives

$$\mathbf{L}\hat{\boldsymbol{\delta}}(x;\omega)r(t) = \mathbf{M}\hat{\boldsymbol{\delta}}(x;\omega)\ddot{r}(t) \quad \text{or} \quad \frac{\mathbf{L}\hat{\boldsymbol{\delta}}(x;\omega)}{\mathbf{M}\hat{\boldsymbol{\delta}}(x;\omega)} = \frac{\ddot{r}(t)}{r(t)} = \lambda \tag{7}$$

where $\lambda = -\omega^2$ should be a negative constant. Thus, we have

$$\ddot{r}(t) + \omega^2 r(t) = 0 \tag{8}$$

with the following solution:

$$r(t) = C_1 e^{-i\omega t} + C_2 e^{i\omega t} \tag{9}$$

from which ω is identified as the circular frequency of a monochromatic wave or of harmonic vibration. For free vibration, we can only take $r = e^{-i\omega t}$ without loss of generality. Thus, the solution to the homogeneous counterpart of Eq. (5) is

$$\boldsymbol{\delta}(x,t) = \hat{\boldsymbol{\delta}}(x;\omega)e^{-i\omega t} \tag{10}$$

where the over caret denotes amplitude or quantity in the frequency domain (the spectral quantity) if Fourier transform is employed.

If the structure is subject to simple harmonic external force vector $\hat{\mathbf{q}}(x;\omega)e^{-i\omega t}$ with ω being the forcing frequency, Eq. (10) denotes the steady-state response [34], while the amplitude vector $\hat{\boldsymbol{\delta}}(x;\omega)$ satisfies the following equation:

$$\mathbf{L}\hat{\boldsymbol{\delta}}(x;\omega) = -\omega^2\mathbf{M}\hat{\boldsymbol{\delta}}(x;\omega) - \hat{\mathbf{q}}(x;\omega) \tag{11}$$

which will be solved by MRRM shown in the next section.

3. Free vibration analysis of complex 3D framed structures with MRRM

MRRM [9–13] has been developed for transient response analysis of planar frames directly based on continuous waveguide models. The solutions to governing equations of a structural member are expressed in terms of traveling wave functions in the frequency domain (Fourier transformed domain). Equilibrium conditions of forces and compatibility conditions of displacements at each joint as well as phase relations of waves in each member are utilized to form a matrix equation to determine the unknown wave amplitudes. The transient response is then obtained as an inverse Fourier integral of the steady-state response over the entire frequency range of $-\infty < \omega < \infty$. For evaluating the early time response, Neumann series expansion is utilized to transform the integrand with an infinite number of poles, which correspond to natural frequencies of the structure, to that without poles. Although MRRM shows certain advantages in transient response analysis, it has not been applied to free vibration problems yet. We will briefly summarize below the main procedure of MRRM for free vibration analysis of a complex 3D structure by following the general notions in Ref. [14].

3.1. Global and local dual coordinates

A representative complex 3D framed structure is shown in Fig. 1. All connecting points of structural members and acting points of concentrated loads are treated as joints in MRRM. The two ends (joints) of a member are denoted as J and K, for instance, and the member will be referred to as JK or KJ. A global coordinate system (X,Y,Z) is used for the whole structure and a pair of local dual coordinate systems (x^{JK}, y^{JK},

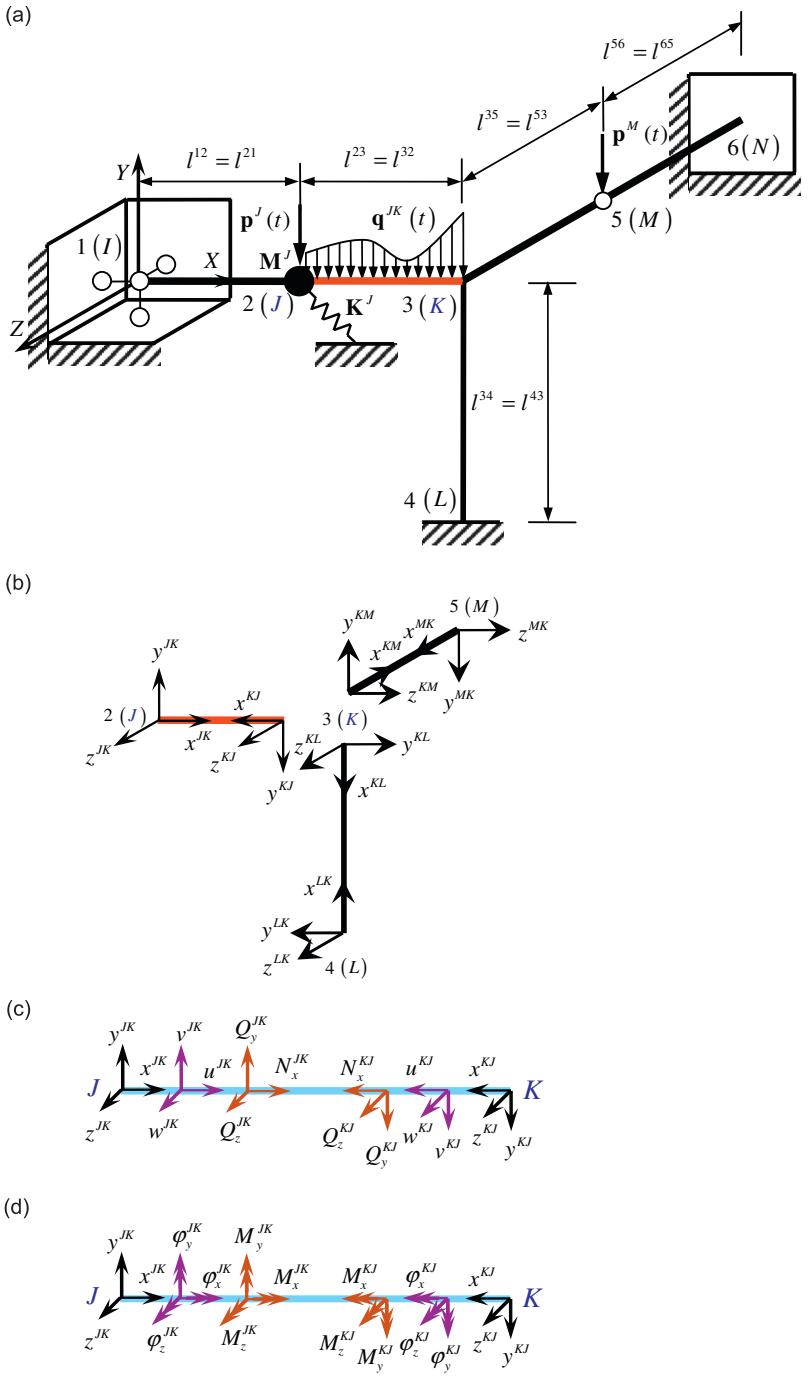

Fig. 1. A representative complex 3D framed structure: (a) geometry of the structure and global coordinates; (b) local dual coordinates of typical structural members; (c) translational displacements and resultant forces in dual coordinates; (d) rotational displacements and moments in dual coordinates.

z^{JK}) and (x^{KJ}, y^{KJ}, z^{KJ}) for each member JK (KJ) with x^{JK} originating from J to K and x^{KJ} from K to J. Thus x^{JK} and x^{KJ} are opposite to each other, and we have

$$x^{KJ} = l^{JK} - x^{JK} \tag{12}$$

at an arbitrary point of a member in dual coordinates. The axes y^{JK}, z^{JK}, y^{KJ} and z^{KJ} coincide with the principal inertia axes of the cross section of the member. The directions of y^{JK} and y^{KJ} are opposite to each other, while those of z^{JK} and z^{KJ} are coincident, following the right-handed screw rule. Note that the use of local dual coordinates for each structural member is unique in MRRM, giving a clear physical image of wave propagation in members and wave scattering at joints. Furthermore, formulations without the problem of numerical instability for high-frequency analysis can be naturally achieved. A detailed comparison between MRRM and MTM, which employs a single coordinate system for each member, can be found in Ref. [13].

To make it clear, superscripts JK or KJ will be affixed to all symbols to indicate the corresponding coordinates. The coordinate systems and the sign convention of physical variables are depicted in Fig. 1. For the discussion of a general framed structure, we denote the total number of joints as n, the total number of members as m, and the number of members connected to joint J as m^J. Clearly, since each member has two ends, we have $\sum_{J=1}^{n} m^J = 2m$.

Hereafter, for the free vibration problem, all symbols without over caret, including the generalized displacement vector $\boldsymbol{\delta}$, generalized force vector $\mathbf{f}$, etc., indicate amplitudes of the respective physical quantities.

3.2. Traveling wave solutions of the reduced governing equations

For free vibration of (free wave propagation in) a uniform member (JK for instance), Eqs. (1)–(4) can be reduced to (with superscripts JK omitted in this subsection)

$$\frac{\mathrm{d}^2 u}{\mathrm{d}x^2} + \frac{\omega^2}{c_1^2} u = 0 \tag{13}$$

for longitudinal wave,

$$\begin{aligned} &\frac{\mathrm{d}^2 v}{\mathrm{d}x^2} - \frac{\mathrm{d}\varphi_z}{\mathrm{d}x} + \frac{\omega^2}{\kappa_y c_2^2} v = 0 \\ &\frac{\mathrm{d}^2 \varphi_z}{\mathrm{d}x^2} + \frac{\kappa_y A c_2^2}{I_z c_1^2}\left(\frac{\mathrm{d}v}{\mathrm{d}x} - \varphi_z\right) + \frac{\omega^2}{c_1^2}\varphi_z = 0 \end{aligned} \tag{14}$$

for flexural wave in xoy plane,

$$\frac{\mathrm{d}^2 w}{\mathrm{d}x^2} - \frac{\mathrm{d}\varphi_y}{\mathrm{d}x} + \frac{\omega^2}{\kappa_z c_2^2} w = 0 \tag{15}$$

$$\frac{\mathrm{d}^2 \varphi_y}{\mathrm{d}x^2} + \frac{\kappa_z A c_2^2}{I_y c_1^2}\left(\frac{\mathrm{d}w}{\mathrm{d}x} - \varphi_y\right) + \frac{\omega^2}{c_1^2}\varphi_y = 0$$

for flexural wave in xoz plane, and

$$\frac{\mathrm{d}^2 \varphi_x}{\mathrm{d}x^2} + \frac{\omega^2}{c_2^2}\varphi_x = 0 \tag{16}$$

for torsional wave. In previous equations, $c_1 = \sqrt{E/\rho}$ and $c_2 = \sqrt{G/\rho}$ are the axial and shear wave velocities, respectively. The solutions to Eqs. (13)–(16) can be written in matrix form as

$$\boldsymbol{\delta}(x;\omega) = \mathbf{A}_\delta(x;\omega)\mathbf{a}(\omega) + \mathbf{D}_\delta(x;\omega)\mathbf{d}(\omega) \tag{17}$$

Accordingly, the generalized force vector is

$$\mathbf{f}(x;\omega) = \mathbf{A}_f(x;\omega)\mathbf{a}(\omega) + \mathbf{D}_f(x;\omega)\mathbf{d}(\omega) \tag{18}$$

In the two expressions, we have introduced the arriving wave vector $\mathbf{a}$ and departing wave vector $\mathbf{d}$ defined as follows:

$$\begin{aligned} \mathbf{a}(\omega) &= [a_1(\omega), a_2(\omega), a_3(\omega), a_4(\omega), a_5(\omega), a_6(\omega)]^{\mathrm{T}} \\ \mathbf{d}(\omega) &= [d_1(\omega), d_2(\omega), d_3(\omega), d_4(\omega), d_5(\omega), d_6(\omega)]^{\mathrm{T}} \end{aligned}$$

with a_j and d_j ($j = 1,2,\ldots,6$) being the arriving wave amplitudes and the departing wave amplitudes of various waves, respectively. The elements of the phase matrices $\mathbf{A}_\delta(x;\omega)$, $\mathbf{D}_\delta(x;\omega)$, $\mathbf{A}_f(x;\omega)$ and $\mathbf{D}_f(x;\omega)$ are given in Appendix B.

3.3. Joint coupling equations and scattering relations

For a perfectly connected joint (J for instance), the equilibrium of forces and the compatibility of displacements lead to

$$\sum_{K=1}^{m^J}(\mathbf{T}^{JK})^{\mathrm{T}}\mathbf{f}^{JK}(0;\omega)=\mathbf{K}_1^J\mathbf{u}^J(\omega),\quad (\mathbf{T}^{JK})^{\mathrm{T}}\boldsymbol{\delta}^{JK}(0;\omega)=\mathbf{u}^J(\omega)\quad (K=1,2,\ldots,m^J) \tag{19}$$

where $\mathbf{u}^J(\omega)$ denotes the generalized displacement vector consisting of three components of translational displacement and another three components of rotational displacement of joint J in the global coordinate system (X, Y, Z), $\mathbf{T}^{JK}$ is the coordinate transformation matrix between the local coordinate system (x^{JK}, y^{JK}, z^{JK}) and the global coordinate system (X, Y, Z), $\mathbf{K}_1^J=\mathbf{K}^J-\omega^2\mathbf{M}^J$ signifies the equivalent stiffness matrix due to the lumped mass and elastic constraint of joint J with $\mathbf{K}^J$ and $\mathbf{M}^J$ being the stiffness and mass matrices, respectively.

Substituting Eqs. (17) and (18) into Eq. (19), yields the local scattering relations at joint J in form of $\mathbf{d}^J=\mathbf{S}^J\mathbf{a}^J$ [9–14], with $\mathbf{S}^J$ being the local scattering matrix, $\mathbf{a}^J=[(\mathbf{a}^{J1})^{\mathrm{T}},(\mathbf{a}^{J2})^{\mathrm{T}},\ldots,(\mathbf{a}^{JK})^{\mathrm{T}},\ldots,(\mathbf{a}^{Jm^J})^{\mathrm{T}}]^{\mathrm{T}}$ and $\mathbf{d}^J=[(\mathbf{d}^{J1})^{\mathrm{T}},(\mathbf{d}^{J2})^{\mathrm{T}},\cdots,(\mathbf{d}^{JK})^{\mathrm{T}},\cdots,(\mathbf{d}^{Jm^J})^{\mathrm{T}}]^{\mathrm{T}}$ the joint arriving and departing wave vectors, respectively. By assembling all joint scattering relations together, we obtain the global scattering relations [9–14]

$$\mathbf{d}=\mathbf{S}\mathbf{a} \tag{20}$$

where $\mathbf{S}=\mathrm{diag}[\mathbf{S}^1,\mathbf{S}^2,\ldots,\mathbf{S}^J,\ldots,\mathbf{S}^n]$ is the global scattering matrix of order $12m\times 12m$, $\mathbf{a}=[(\mathbf{a}^1)^{\mathrm{T}},(\mathbf{a}^2)^{\mathrm{T}},\ldots,(\mathbf{a}^J)^{\mathrm{T}},\ldots,(\mathbf{a}^n)^{\mathrm{T}}]^{\mathrm{T}}$ and $\mathbf{d}=[(\mathbf{d}^1)^{\mathrm{T}},(\mathbf{d}^2)^{\mathrm{T}},\ldots,(\mathbf{d}^J)^{\mathrm{T}},\ldots,(\mathbf{d}^n)^{\mathrm{T}}]^{\mathrm{T}}$ are respectively the global arriving and departing wave vectors of order $12m\times 1$.

It is noted that, if there is pin-connected joint (such as joint M of the frame shown in Fig. 1), the compatibility conditions about rotation should be replaced by the vanishing of moments at that joint, $M_i^{JK}(0;\omega)=0\quad (K=1,2,\ldots,m^J)$. Meanwhile, the Euler's equation of angular momentum of the joint in the first equation of Eq. (19) should be removed. For other kinds of joint, the equilibrium equations and the compatibility conditions should also be rewritten according to the property of the joint [14]. In any case, the joint scattering relations as well as the global scattering relations can be written in the same form as described above.

3.4. Compatibility conditions of physical variables in local dual coordinates and phase relations

The generalized displacement and force vectors in local dual coordinates for an arbitrary member JK (KJ) should satisfy

$$\boldsymbol{\delta}^{JK}(x^{JK})=\mathbf{T}_\delta\boldsymbol{\delta}^{KJ}(l^{JK}-x^{JK}),\quad \mathbf{f}^{JK}(x^{JK})=\mathbf{T}_f\mathbf{f}^{KJ}(l^{JK}-x^{JK}) \tag{22}$$

where

$$\mathbf{T}_\delta=\mathrm{diag}[-1,-1,1,-1,-1,1],\quad \mathbf{T}_f=\mathrm{diag}[1,1,-1,1,1,-1] \tag{23}$$

It is obvious that $\mathbf{T}_\delta\mathbf{T}_f=-\mathbf{I}_{6\times 6}$, here $\mathbf{I}_{6\times 6}$ is a unit matrix of order 6. Substitution of Eq. (17) into the first of Eq. (22) gives the local phase relations $\mathbf{a}^{JK}=\mathbf{P}^{JK}(l^{JK};\omega)\mathbf{d}^{JK}$ and $\mathbf{a}^{KJ}=\mathbf{P}^{JK}(l^{JK};\omega)\mathbf{d}^{JK}$ for member JK. These can be assembled in sequence to obtain the joint phase relations $\mathbf{a}^J=\mathbf{P}^J(\omega)\bar{\mathbf{d}}^J$ for joint J and the global phase relations for the whole structure

$$\mathbf{a}=\mathbf{P}(\omega)\bar{\mathbf{d}}=\mathbf{P}(\omega)\mathbf{U}\mathbf{d} \tag{24}$$

with $\mathbf{P}^J=\mathrm{diag}[\mathbf{P}^{J1},\mathbf{P}^{J2},\ldots,\mathbf{P}^{JK},\ldots,\mathbf{P}^{Jm^J}]$ and $\mathbf{P}=\mathrm{diag}[\mathbf{P}^1,\mathbf{P}^2,\ldots,\mathbf{P}^J,\ldots,\mathbf{P}^n]$ being the joint and global phase matrices. The departing wave vector $\bar{\mathbf{d}}=[(\bar{\mathbf{d}}^1)^{\mathrm{T}},(\bar{\mathbf{d}}^2)^{\mathrm{T}},\ldots,(\bar{\mathbf{d}}^J)^{\mathrm{T}},\ldots,(\bar{\mathbf{d}}^n)^{\mathrm{T}}]^{\mathrm{T}}$, where

$\bar{\mathbf{d}}^J = [(\mathbf{d}^{1J})^T, (\mathbf{d}^{2J})^T, \ldots, (\mathbf{d}^{KJ})^T, \ldots, (\mathbf{d}^{m'J})^T]^T$, has the same elements as $\mathbf{d}$ but with a different sequence. $\mathbf{U}$ is the permutation matrix of order $12m \times 12m$ with only one element of unit (1) in each row and column and the others being zero; it is introduced to take account of the different sequences of elements in $\mathbf{d}$ and $\bar{\mathbf{d}}$.

3.5. Reverberation-ray matrix and frequency equation

Substituting Eq. (24) into Eq. (20) or substituting Eq. (20) into Eq. (24) gives

$$[\mathbf{I} - \mathbf{R}(\omega)]\mathbf{d}(\omega) = \mathbf{0}, \quad [\mathbf{I} - \mathbf{R}'(\omega)]\mathbf{a}(\omega) = \mathbf{0} \tag{25a,b}$$

where $\mathbf{R}(\omega) \equiv \mathbf{S}(\omega)\mathbf{P}(\omega)\mathbf{U}$ is the reverberation-ray matrix previously defined in Refs. [9–14], $\mathbf{R}'(\omega) \equiv \mathbf{P}(\omega)\mathbf{U}\mathbf{S}(\omega)$ is another form of reverberation-ray matrix. Both are complex, sparse, and unsymmetric matrices, and describe the physical essence of wave scattering at all joints and wave traveling along all members. However, the matrix $\mathbf{R}$, formed when the departing wave vector is treated as unknown, indicates that wave traveling along members takes place first, then followed by wave scattering at joints, while the matrix $\mathbf{R}'$, formed when the arriving wave vector is the unknown, implies that wave scattering at joints happens first, and the traveling of waves along members then follows. This understanding is very important when using the Neumann series expansion to perform the inverse Fourier integration for transient analysis, see the discussion on causality of wave propagation associated with MRRM in Ref. [11]. Since we only use MRRM to perform the free vibration analysis in this work, there is no difference between the two mathematically equivalent formulations given in Eq. (25). For non-trivial solution to exist, the coefficient determinant of Eq. (25a) or (25b) should vanish. Taking Eq. (25a) for instance, we have

$$|\mathbf{I} - \mathbf{R}(\omega)| = 0 \tag{26}$$

which is the frequency equation of the structure.

3.6. Natural frequencies and normal modes analysis

To find the roots of Eq. (26), i.e. the natural frequencies of the structure, ω_r ($r = 1,2,3,\ldots$), a hybrid searching scheme is employed, which combines the bisection method and golden section method and performs very well for planar frames as demonstrated in Ref. [35]. The associated natural modes can be calculated based on the associated non-trivial solutions $\mathbf{d}_r$ ($r = 1,2,3,\ldots$) of Eq. (25) [36], which are obtained in the following way.

(i) For a certain natural frequency ω_r, the rank of the coefficient matrix $\mathbf{I}-\mathbf{R}(\omega_r)$ is first calculated. Denote it as r_c. Then $n_c = 12m-r_c$ is equal to the number of coincident frequencies of ω_r. Find out the linearly independent set $\mathbf{d}_0$, a column matrix of order $r_c \times 1$, and rewrite Eq. (25) as

$$\mathbf{G}_0\mathbf{d}_0 = \mathbf{G}_c\mathbf{d}_c \tag{27}$$

where $\mathbf{G}_0$ is a sub-matrix of order $r_c \times r_c$ and rank r_c, which is a principle minor of $|\mathbf{I} - \mathbf{R}|$; $\mathbf{G}_c$ is a rectangular coefficient matrix of order $r_c \times n_c$, which is complementary to $\mathbf{G}_0$; $\mathbf{d}_c$, of order $n_c \times 1$, is the complementary subset to $\mathbf{d}_0$ of the entire column $\mathbf{d}$. The elements of $\mathbf{d}_c$ are understood to be free variables and independent of each other, while the elements of $\mathbf{d}_0$ are determined from those of $\mathbf{d}_c$ by Eq. (27).

(ii) Let only one element in $\mathbf{d}_c$ equal 1 and others 0, and solve for $\mathbf{d}_0$ from Eq. (27). This determines one non-trivial solution corresponding to ω_r.

(iii) If $n_c > 1$, repeat step (ii) but let a different element be 1. The procedure are conducted n_c times and n_c independent non-trivial solutions can be obtained for the n_c coincident frequencies of ω_r.

After $\mathbf{d}$ is obtained, $\mathbf{a}$ is easily calculated from Eq. (24). The generalized displacements are then calculated accordingly from Eq. (17). These displacement vectors are n_c linearly independent natural modes for n_c coincident frequencies of ω_r. They can be further orthogonalized by the scheme of Schmidt orthogonalization. Thus we can always assume that the modes for coincident frequencies are orthogonal with each other.

In the following section, we will further prove that the modes for non-coincident frequencies are mutually orthogonal in both the dual and single coordinates. Based on the orthogonality of different natural modes, the mode superposition method for transient response analysis can be formulated accordingly.

4. Orthogonality of normal modes and forced vibration analysis

Transient response of structures can be obtained conveniently by the mode superposition method if the natural modes are orthogonal with each other. In a previous paper [35], we have established the orthogonality of natural modes for planar framed structures with optional lumped masses and/or elastic supports. In this paper, a different procedure which utilizes Betti's reciprocity theorem [32] will be adopted for the establishment of orthogonality of natural modes for complex 3D framed structures. Similar discussion has been given in Ref. [1] to demonstrate the orthogonality of modes of axial and flexural vibrations for a simple rod.

4.1. Orthogonality of natural modes

Assume $\boldsymbol{\delta}_i^{JK}=[u_i^{JK},v_i^{JK},w_i^{JK},\varphi_{xi}^{JK},\varphi_{yi}^{JK},\varphi_{zi}^{JK}]^{\mathrm{T}}$and $\boldsymbol{\delta}_j^{JK}=[u_j^{JK},v_j^{JK},w_j^{JK},\varphi_{xj}^{JK},\varphi_{yj}^{JK},\varphi_{zj}^{JK}]^{\mathrm{T}}$ are displacement vectors of member JK in coordinates $(x,\ y,\ z)^{JK}$ corresponding to two different natural frequencies ω_i and ω_j $(\omega_{i,j}\neq 0)$, while $\boldsymbol{\delta}_i^{KJ}=[u_i^{KJ},v_i^{KJ},w_i^{KJ},\varphi_{xi}^{KJ},\varphi_{yi}^{KJ},\varphi_{zi}^{KJ}]^{\mathrm{T}}$and $\boldsymbol{\delta}_j^{KJ}=[u_j^{KJ},v_j^{KJ},w_j^{KJ},\varphi_{xj}^{KJ},\varphi_{yj}^{KJ},\varphi_{zj}^{KJ}]^{\mathrm{T}}$ are those in dual coordinates $(x,\ y,\ z)^{KJ}$. For free vibration problem, applying Betti's reciprocity theorem [32] to the segment from 0 to x^{JK} $(0<x^{JK}\leqslant l^{JK})$ of member JK in coordinate $(x,\ y,\ z)^{JK}$ gives

$$\int_0^{x^{JK}}\left(\boldsymbol{\delta}_i^{JK}\right)^{\mathrm{T}}\mathbf{f}_{Ij}^{JK}\,\mathrm{d}x+\left[\left(\boldsymbol{\delta}_i^{JK}\right)^{\mathrm{T}}\mathbf{f}_j^{JK}\right]_0-\left[\left(\boldsymbol{\delta}_i^{JK}\right)^{\mathrm{T}}\mathbf{f}_j^{JK}\right]_{x^{JK}}$$
$$=\int_0^{x^{JK}}\left(\boldsymbol{\delta}_j^{JK}\right)^{\mathrm{T}}\mathbf{f}_{Ii}^{JK}\,\mathrm{d}x+\left[\left(\boldsymbol{\delta}_j^{JK}\right)^{\mathrm{T}}\mathbf{f}_i^{JK}\right]_0-\left[\left(\boldsymbol{\delta}_j^{JK}\right)^{\mathrm{T}}\mathbf{f}_i^{JK}\right]_{x^{JK}} \tag{28}$$

where $\mathbf{f}_{Ii}^{JK}$ and $\mathbf{f}_{Ij}^{JK}$ are given by

$$\mathbf{f}_{Ii}^{JK}=-\omega_i^2\int_0^{x^{JK}}\mathbf{M}^{JK}\boldsymbol{\delta}_i^{JK}\,\mathrm{d}x,\quad \mathbf{f}_{Ij}^{JK}=-\omega_j^2\int_0^{x^{JK}}\mathbf{M}^{JK}\boldsymbol{\delta}_j^{JK}\,\mathrm{d}x \tag{29}$$

Note that

$$\int_0^{x^{JK}}\left(\boldsymbol{\delta}_i^{JK}\right)^{\mathrm{T}}\mathbf{M}^{JK}\boldsymbol{\delta}_j^{JK}\,\mathrm{d}x=\int_0^{x^{JK}}\left(\boldsymbol{\delta}_j^{JK}\right)^{\mathrm{T}}\mathbf{M}^{JK}\boldsymbol{\delta}_i^{JK}\,\mathrm{d}x$$
$$=\int_0^{x^{JK}}\rho^{JK}(x)\left[u_j^{JK}A^{JK}(x)u_i^{JK}+v_j^{JK}A^{JK}(x)v_i^{JK}+w_j^{JK}A^{JK}(x)w_i^{JK}\right]\mathrm{d}x$$
$$+\int_0^{x^{JK}}\rho^{JK}(x)\left[\varphi_{xj}^{JK}I_x^{JK}(x)\varphi_{xi}^{JK}+\varphi_{yj}^{JK}I_y^{JK}(x)\varphi_{yi}^{JK}+\varphi_{zj}^{JK}I_z^{JK}(x)\varphi_{zi}^{JK}\right]\mathrm{d}x \tag{30}$$

Then from Eq. (28) we have

$$(\omega_i^2-\omega_j^2)\int_0^{x^{JK}}\left(\boldsymbol{\delta}_i^{JK}\right)^{\mathrm{T}}\mathbf{M}^{JK}\boldsymbol{\delta}_j^{JK}\,\mathrm{d}x=\left[\left(\boldsymbol{\delta}_i^{JK}\right)^{\mathrm{T}}\mathbf{f}_j^{JK}-\left(\boldsymbol{\delta}_j^{JK}\right)^{\mathrm{T}}\mathbf{f}_i^{JK}\right]_0^{x^{JK}}\equiv\boldsymbol{\Delta}_{ij}^{JK}\Big|_0^{x^{JK}} \tag{31}$$

Similar equations can be established for the segment from 0 to $l^{JK}-x^{JK}$ of member JK in coordinates $(x,\ y,\ z)^{KJ}$. Summing up equations for all m members in the dual coordinates, we obtain

$$(\omega_i^2-\omega_j^2)\left\{\sum_{k=1}^{m}\left[\int_0^{x^{JK}}\left(\boldsymbol{\delta}_i^{JK}\right)^{\mathrm{T}}\mathbf{M}^{JK}\boldsymbol{\delta}_j^{JK}\,\mathrm{d}x\right]+\sum_{k=1}^{m}\left[\int_0^{l^{JK}-x^{JK}}\left(\boldsymbol{\delta}_i^{KJ}\right)^{\mathrm{T}}\mathbf{M}^{KJ}\boldsymbol{\delta}_j^{KJ}\,\mathrm{d}x\right]\right\}$$
$$=\sum_{k=1}^{m}\left[\boldsymbol{\Delta}_{ij}^{JK}(x^{JK})+\boldsymbol{\Delta}_{ij}^{KJ}(l^{JK}-x^{JK})\right]-\sum_{k=1}^{m}\left[\boldsymbol{\Delta}_{ij}^{JK}(0)+\boldsymbol{\Delta}_{ij}^{KJ}(0)\right] \tag{32}$$

where k is the sequence number of member JK (or KJ) in the total m members. In this paper, we sometimes also affix a single subscript to a material/geometric parameter or even an operator matrix of member (say JK), such as $l_k \equiv l^{JK}$, $\mathbf{M}_k \equiv \mathbf{M}^{JK}$ and $\mathbf{L}_k \equiv \mathbf{L}^{JK}$. In view of the compatibility conditions of physical variables in dual coordinates of all m members as shown in Eq. (22) and the joint coupling equations of all n joints as given in Eq. (19) (or similar [35]), Eq. (32) further gives

$$\begin{aligned}(\omega_i^2-\omega_j^2)\left\{\sum_{k=1}^{m}\left[\int_0^{x^{JK}}\left(\boldsymbol{\delta}_i^{JK}\right)^{\mathrm{T}}\mathbf{M}^{JK}\boldsymbol{\delta}_j^{JK}\,\mathrm{d}x\right]+\sum_{k=1}^{m}\left[\int_0^{l^{JK}-x^{JK}}\left(\boldsymbol{\delta}_i^{KJ}\right)^{\mathrm{T}}\mathbf{M}^{KJ}\boldsymbol{\delta}_j^{KJ}\,\mathrm{d}x\right]\right\}\\ =-(\omega_i^2-\omega_j^2)\sum_{J=1}^{n}\left[\left(\mathbf{u}_i^J\right)^{\mathrm{T}}\mathbf{M}^J\mathbf{u}_j^J\right]\end{aligned} \tag{33}$$

which has the same form as that given in Ref. [35] for planar frames. Eq. (33) indicates that

$$(\omega_i^2-\omega_j^2)\left\{\sum_{k=1}^{m}\left[\int_0^{x^{JK}}\left(\boldsymbol{\delta}_i^{JK}\right)^{\mathrm{T}}\mathbf{M}^{JK}\boldsymbol{\delta}_j^{JK}\,\mathrm{d}x\right]+\sum_{k=1}^{m}\left[\int_0^{l^{JK}-x^{JK}}\left(\boldsymbol{\delta}_i^{KJ}\right)^{\mathrm{T}}\mathbf{M}^{KJ}\boldsymbol{\delta}_j^{KJ}\,\mathrm{d}x\right]+\sum_{J=1}^{n}\left[\left(\mathbf{u}_i^J\right)^{\mathrm{T}}\mathbf{M}^J\mathbf{u}_j^J\right]\right\}=0 \tag{34}$$

For $\omega_i \neq \omega_j$, we have

$$\sum_{k=1}^{m}\left[\int_0^{x^{JK}}\left(\boldsymbol{\delta}_i^{JK}\right)^{\mathrm{T}}\mathbf{M}^{JK}\boldsymbol{\delta}_j^{JK}\,\mathrm{d}x\right]+\sum_{k=1}^{m}\left[\int_0^{l^{JK}-x^{JK}}\left(\boldsymbol{\delta}_i^{KJ}\right)^{\mathrm{T}}\mathbf{M}^{KJ}\boldsymbol{\delta}_j^{KJ}\,\mathrm{d}x\right]+\sum_{J=1}^{n}\left[\left(\mathbf{u}_i^J\right)^{\mathrm{T}}\mathbf{M}^J\mathbf{u}_j^J\right]=0 \tag{35}$$

Furthermore, from Eq. (19) we obtain

$$-\omega_j^2\mathbf{M}^J\mathbf{u}_j^J=\sum_{K=1}^{m^J}(\mathbf{T}^{JK})^{\mathrm{T}}\mathbf{f}_j^{JK}(0)-\mathbf{K}^J\mathbf{u}_j^J \tag{36}$$

Pre-multiplying by $\left(\mathbf{u}_i^J\right)^{\mathrm{T}}=[(\mathbf{T}^{JK})^{\mathrm{T}}\boldsymbol{\delta}_i^{JK}(0)]^{\mathrm{T}}$ and summating over all n joints, we arrive at

$$-\omega_j^2\sum_{J=1}^{n}\left[\left(\mathbf{u}_i^J\right)^{\mathrm{T}}\mathbf{M}^J\mathbf{u}_j^J\right]=\sum_{J=1}^{n}\sum_{K=1}^{m^J}\left\{[\boldsymbol{\delta}_i^{JK}(0)]^{\mathrm{T}}\mathbf{f}_j^{JK}(0)\right\}-\sum_{J=1}^{n}\left[\left(\mathbf{u}_i^J\right)^{\mathrm{T}}\mathbf{K}^J\mathbf{u}_j^J\right] \tag{37a}$$

$$-\omega_j^2\sum_{J=1}^{n}\left[\left(\mathbf{u}_i^J\right)^{\mathrm{T}}\mathbf{M}^J\mathbf{u}_j^J\right]=\sum_{J=1}^{n}\sum_{K=1}^{m^J}\left\{[\boldsymbol{\delta}_i^{KJ}(0)]^{\mathrm{T}}\mathbf{f}_j^{KJ}(0)\right\}-\sum_{J=1}^{n}\left[\left(\mathbf{u}_i^J\right)^{\mathrm{T}}\mathbf{K}^J\mathbf{u}_j^J\right] \tag{37b}$$

Although Eq. (37) is derived based on Eq. (19) for a perfectly rigid joint, it is also applicable to pinned joints and other elastically supported joints as shown in Ref. [35]. Moreover, from the homogenous counterpart of Eq. (11) we have

$$\begin{aligned}\int_0^{x^{JK}}\left(\boldsymbol{\delta}_i^{JK}\right)^{\mathrm{T}}\mathbf{L}^{JK}\boldsymbol{\delta}_j^{JK}\,\mathrm{d}x&=-\omega_j^2\int_0^{x^{JK}}\left(\boldsymbol{\delta}_i^{JK}\right)^{\mathrm{T}}\mathbf{M}^{JK}\boldsymbol{\delta}_j^{JK}\,\mathrm{d}x\\ \int_0^{l^{JK}-x^{JK}}\left(\boldsymbol{\delta}_i^{KJ}\right)^{\mathrm{T}}\mathbf{L}^{KJ}\boldsymbol{\delta}_j^{KJ}\,\mathrm{d}x&=-\omega_j^2\int_0^{l^{JK}-x^{JK}}\left(\boldsymbol{\delta}_i^{KJ}\right)^{\mathrm{T}}\mathbf{M}^{KJ}\boldsymbol{\delta}_j^{KJ}\,\mathrm{d}x\end{aligned} \tag{38}$$

Substitution of Eqs. (37) and (38) into Eq. (35) gives

$$\begin{aligned}&\sum_{k=1}^{m}\left[\int_0^{x^{JK}}\left(\boldsymbol{\delta}_i^{JK}\right)^{\mathrm{T}}\mathbf{L}^{JK}\boldsymbol{\delta}_j^{JK}\,\mathrm{d}x\right]+\sum_{k=1}^{m}\left[\int_0^{l^{JK}-x^{JK}}\left(\boldsymbol{\delta}_i^{KJ}\right)^{\mathrm{T}}\mathbf{L}^{KJ}\boldsymbol{\delta}_j^{KJ}\,\mathrm{d}x\right]\\ &\quad+\sum_{J=1}^{n}\sum_{K=1}^{m^J}\left\{[\boldsymbol{\delta}_i^{JK}(0)]^{\mathrm{T}}\mathbf{f}_j^{JK}(0)\right\}-\sum_{J=1}^{n}\left[\left(\mathbf{u}_i^J\right)^{\mathrm{T}}\mathbf{K}^J\mathbf{u}_j^J\right]=0\end{aligned} \tag{39a}$$

$$\sum_{k=1}^{m}\left[\int_0^{x^{JK}}\left(\boldsymbol{\delta}_i^{JK}\right)^{\mathrm{T}}\mathbf{L}^{JK}\boldsymbol{\delta}_j^{JK}\,\mathrm{d}x\right]+\sum_{k=1}^{m}\left[\int_0^{l^{JK}-x^{JK}}\left(\boldsymbol{\delta}_i^{KJ}\right)^{\mathrm{T}}\mathbf{L}^{KJ}\boldsymbol{\delta}_j^{KJ}\,\mathrm{d}x\right]$$
$$+\sum_{J=1}^{n}\sum_{K=1}^{m^J}\left\{\left[\boldsymbol{\delta}_i^{KJ}(0)\right]^{\mathrm{T}}\mathbf{f}_j^{KJ}(0)\right\}-\sum_{J=1}^{n}\left[\left(\mathbf{u}_i^J\right)^{\mathrm{T}}\mathbf{K}^J\mathbf{u}_j^J\right]=0 \tag{39b}$$

When $x^{JK}=l^{JK}\equiv l_k$, Eqs. (35) and (39a) become

$$\sum_{k=1}^{m}\left[\int_0^{l_k}\left(\boldsymbol{\delta}_i^{JK}\right)^{\mathrm{T}}\mathbf{M}^{JK}\boldsymbol{\delta}_j^{JK}\,\mathrm{d}x\right]+\sum_{J=1}^{n}\left[\left(\mathbf{u}_i^J\right)^{\mathrm{T}}\mathbf{M}^J\mathbf{u}_j^J\right]=0 \tag{40}$$

$$\sum_{k=1}^{m}\left[\int_0^{l_k}\left(\boldsymbol{\delta}_i^{JK}\right)^{\mathrm{T}}\mathbf{L}^{JK}\boldsymbol{\delta}_j^{JK}\,\mathrm{d}x\right]+\sum_{J=1}^{n}\sum_{K=1}^{m^J}\left\{\left[\boldsymbol{\delta}_i^{JK}(0)\right]^{\mathrm{T}}\mathbf{f}_j^{JK}(0)\right\}-\sum_{J=1}^{n}\left[\left(\mathbf{u}_i^J\right)^{\mathrm{T}}\mathbf{K}^J\mathbf{u}_j^J\right]=0 \tag{41}$$

where only the coordinate system $(x, y, z)^{JK}$ is involved. As shown in Eqs. (35), (39), (40) and (41), two different natural modes are orthogonal in both the dual coordinates and the single coordinates in a global sense.

Now the orthogonal conditions of natural modes can be stated as

$$\sum_{k=1}^{m}\left[\int_0^{x^{JK}}\left(\boldsymbol{\delta}_i^{JK}\right)^{\mathrm{T}}\mathbf{M}^{JK}\boldsymbol{\delta}_j^{JK}\,\mathrm{d}x\right]+\sum_{k=1}^{m}\left[\int_0^{l^{JK}-x^{JK}}\left(\boldsymbol{\delta}_i^{KJ}\right)^{\mathrm{T}}\mathbf{M}^{KJ}\boldsymbol{\delta}_j^{KJ}\,\mathrm{d}x\right]+\sum_{J=1}^{n}\left[\left(\mathbf{u}_i^J\right)^{\mathrm{T}}\mathbf{M}^J\mathbf{u}_j^J\right]=M_j\delta_{ji} \tag{42}$$

$$\sum_{k=1}^{m}\left[\int_0^{l_k}\left(\boldsymbol{\delta}_i^{JK}\right)^{\mathrm{T}}\mathbf{M}^{JK}\boldsymbol{\delta}_j^{JK}\,\mathrm{d}x\right]+\sum_{J=1}^{n}\left[\left(\mathbf{u}_i^J\right)^{\mathrm{T}}\mathbf{M}^J\mathbf{u}_j^J\right]=M_j\delta_{ji} \tag{43}$$

in dual and single coordinates, respectively, where

$$\begin{aligned}M_j&=\sum_{k=1}^{m}\left[\int_0^{x^{JK}}\left(\boldsymbol{\delta}_j^{JK}\right)^{\mathrm{T}}\mathbf{M}^{JK}\boldsymbol{\delta}_j^{JK}\,\mathrm{d}x\right]+\sum_{k=1}^{m}\left[\int_0^{l^{JK}-x^{JK}}\left(\boldsymbol{\delta}_j^{KJ}\right)^{\mathrm{T}}\mathbf{M}^{KJ}\boldsymbol{\delta}_j^{KJ}\,\mathrm{d}x\right]+\sum_{J=1}^{n}\left[\left(\mathbf{u}_j^J\right)^{\mathrm{T}}\mathbf{M}^J\mathbf{u}_j^J\right]\\&=\sum_{k=1}^{m}\left[\int_0^{l_k}\left(\boldsymbol{\delta}_j^{JK}\right)^{\mathrm{T}}\mathbf{M}^{JK}\boldsymbol{\delta}_j^{JK}\,\mathrm{d}x\right]+\sum_{J=1}^{n}\left[\left(\mathbf{u}_j^J\right)^{\mathrm{T}}\mathbf{M}^J\mathbf{u}_j^J\right]\end{aligned} \tag{44}$$

is the norm of the natural mode, i.e. the generalized mass, corresponding to the frequency ω_j, and δ_{ji} is the Kronecker delta. The derivation of the second equality in Eq. (44) was given in Ref. [35].

The conditions of orthogonality of natural modes can also be represented as

$$\sum_{k=1}^{m}\left[\int_0^{x^{JK}}\left(\boldsymbol{\delta}_i^{JK}\right)^{\mathrm{T}}\mathbf{L}^{JK}\boldsymbol{\delta}_j^{JK}\,\mathrm{d}x\right]+\sum_{k=1}^{m}\left[\int_0^{l^{JK}-x^{JK}}\left(\boldsymbol{\delta}_i^{KJ}\right)^{\mathrm{T}}\mathbf{L}^{KJ}\boldsymbol{\delta}_j^{KJ}\,\mathrm{d}x\right]$$
$$+\sum_{J=1}^{n}\sum_{K=1}^{m^J}\left\{\left[\boldsymbol{\delta}_i^{JK}(0)\right]^{\mathrm{T}}\mathbf{f}_j^{JK}(0)\right\}-\sum_{J=1}^{n}\left[\left(\mathbf{u}_i^J\right)^{\mathrm{T}}\mathbf{K}^J\mathbf{u}_j^J\right]=-K_j\delta_{ji} \tag{45}$$

$$\sum_{k=1}^{m}\left[\int_0^{l_k}\left(\boldsymbol{\delta}_i^{JK}\right)^{\mathrm{T}}\mathbf{L}^{JK}\boldsymbol{\delta}_j^{JK}\,\mathrm{d}x\right]+\sum_{J=1}^{n}\sum_{K=1}^{m^J}\left\{\left[\boldsymbol{\delta}_i^{JK}(0)\right]^{\mathrm{T}}\mathbf{f}_j^{JK}(0)\right\}-\sum_{J=1}^{n}\left[\left(\mathbf{u}_i^J\right)^{\mathrm{T}}\mathbf{K}^J\mathbf{u}_j^J\right]=-K_j\delta_{ji} \tag{46}$$

in dual and single coordinates, respectively, where

$$K_j = -\sum_{k=1}^{m}\int_0^{x^{JK}}\left[\left(\boldsymbol{\delta}_j^{JK}\right)^{\mathrm{T}}\mathbf{L}^{JK}\boldsymbol{\delta}_j^{JK}\right]\mathrm{d}x - \sum_{k=1}^{m}\int_0^{l^{JK}-x^{JK}}\left[\left(\boldsymbol{\delta}_j^{KJ}\right)^{\mathrm{T}}\mathbf{L}^{KJ}\boldsymbol{\delta}_j^{KJ}\right]\mathrm{d}x$$
$$-\sum_{J=1}^{n}\sum_{K=1}^{m^J}\left\{\left[\boldsymbol{\delta}_j^{JK}(0)\right]^{\mathrm{T}}\mathbf{f}_j^{JK}(0)\right\} + \sum_{J=1}^{n}\left[\left(\mathbf{u}_j^J\right)^{\mathrm{T}}\mathbf{K}^J\mathbf{u}_j^J\right]$$
$$= -\sum_{k=1}^{m}\int_0^{l_k}\left[\left(\boldsymbol{\delta}_j^{JK}\right)^{\mathrm{T}}\mathbf{L}^{JK}\boldsymbol{\delta}_j^{JK}\right]\mathrm{d}x - \sum_{J=1}^{n}\sum_{K=1}^{m^J}\left\{\left[\boldsymbol{\delta}_j^{JK}(0)\right]^{\mathrm{T}}\mathbf{f}_j^{JK}(0)\right\} + \sum_{J=1}^{n}\left[\left(\mathbf{u}_j^J\right)^{\mathrm{T}}\mathbf{K}^J\mathbf{u}_j^J\right] \tag{47}$$

is the generalized stiffness corresponding to the frequency ω_j. The relation between the generalized mass and generalized stiffness of complex 3D structures is identical to that of a multi-degree-of-freedom (mdof) system, viz.

$$K_j = \omega_j^2 M_j \quad (j = 1, 2, \ldots, \infty) \tag{48}$$

4.2. Mode superposition based on mode orthogonality

Having established the orthogonality of natural modes as given in Eqs. (42) and (43) as well as (45) and (46), we can develop the mode superposition method for transient response analysis of complex 3D framed structures. The procedure is almost the same as that outlined in Ref. [35] for planar frames, and hence only some key formulations are given in the following. Changing the symbols $\boldsymbol{\delta}^{JK}$, $\boldsymbol{\delta}_i^{JK}$ and $\boldsymbol{\delta}_j^{JK}$ to $\boldsymbol{\delta}_k$, $\boldsymbol{\delta}_{ki}$ and $\boldsymbol{\delta}_{kj}$, respectively, we may express the displacement responses of member k in terms of natural modes of the structure

$$\boldsymbol{\delta}_k(x,t) = \sum_{j=1}^{\infty}\boldsymbol{\delta}_{kj}(x)r_j(t) \tag{49}$$

Note that the new symbols with a single subscript k replacing the double superscripts JK are more convenient to be used in the mode superposition method. Then, from the governing equations (Eq. (5)) of all m members, we can derive

$$\sum_{j=1}^{\infty}\left\{r_j(t)\sum_{k=1}^{m}\left[\int_0^{l_k}\boldsymbol{\delta}_{ki}^{\mathrm{T}}(x)\mathbf{L}_k\boldsymbol{\delta}_{kj}(x)\,\mathrm{d}x\right]\right\}$$
$$= \sum_{j=1}^{\infty}\left\{\ddot{r}_j(t)\sum_{k=1}^{m}\left[\int_0^{l_k}\boldsymbol{\delta}_{ki}^{\mathrm{T}}(x)\mathbf{M}_k\boldsymbol{\delta}_{kj}(x)\,\mathrm{d}x\right]\right\} - \sum_{k=1}^{m}\left[\int_0^{l_k}\boldsymbol{\delta}_{ki}^{\mathrm{T}}(x)\mathbf{q}_k(x,t)\,\mathrm{d}x\right] \tag{50}$$

in which the effect of distributed force $\mathbf{q}_k(x, t)$ is involved. From the joint coupling equations at all joints we can obtain

$$\sum_{j=1}^{\infty}r_j(t)\left\{\sum_{J=1}^{n}\sum_{K=1}^{m^J}\left[\left(\boldsymbol{\delta}_i^{JK}(0)\right)^{\mathrm{T}}\mathbf{f}_j^{JK}(0)\right] - \sum_{J=1}^{n}\left[\left(\mathbf{u}_i^J\right)^{\mathrm{T}}\mathbf{K}^J\mathbf{u}_j^J\right]\right\}$$
$$= \sum_{j=1}^{\infty}\ddot{r}_j(t)\left\{\sum_{J=1}^{n}\left[\left(\mathbf{u}_i^J\right)^{\mathrm{T}}\mathbf{M}^J\mathbf{u}_j^J\right]\right\} - \sum_{J=1}^{n}\left[\left(\mathbf{u}_i^J\right)^{\mathrm{T}}\mathbf{p}^J(t)\right] \tag{51}$$

Eqs. (50) and (51) can be combined to give

$$\sum_{j=1}^{\infty}r_j(t)\left\{\sum_{k=1}^{m}\int_0^{l_k}\left[\boldsymbol{\delta}_{ki}^{\mathrm{T}}(x)\mathbf{L}_k\boldsymbol{\delta}_{kj}(x)\right]\mathrm{d}x + \sum_{J=1}^{n}\sum_{K=1}^{m^J}\left[\left(\boldsymbol{\delta}_i^{JK}(0)\right)^{\mathrm{T}}\mathbf{f}_j^{JK}(0)\right] - \sum_{J=1}^{n}\left[\left(\mathbf{u}_i^J\right)^{\mathrm{T}}\mathbf{K}^J\mathbf{u}_j^J\right]\right\}$$
$$= \sum_{j=1}^{\infty}\ddot{r}_j(t)\left\{\sum_{k=1}^{m}\int_0^{l_k}\left[\boldsymbol{\delta}_{ki}^{\mathrm{T}}(x)\mathbf{M}_k\boldsymbol{\delta}_{kj}(x)\right]\mathrm{d}x + \sum_{J=1}^{n}\left[\left(\mathbf{u}_i^J\right)^{\mathrm{T}}\mathbf{M}^J\mathbf{u}_j^J\right]\right\}$$

$$-\sum_{k=1}^{m}\int_0^{l_k}\boldsymbol{\delta}_{ki}^{\mathrm{T}}(x)\mathbf{q}_k(x,t)\mathrm{d}x-\sum_{J=1}^{n}\left[\left(\mathbf{u}_i^J\right)^{\mathrm{T}}\mathbf{p}^J(t)\right] \tag{52}$$

In view of the orthogonality conditions in Eqs. (43) and (46), we finally derive a single ordinary differential equation for $r_j(t)$, that is

$$M_j\ddot{r}_j(t)+\omega_j^2M_jr_j(t)=\sum_{k=1}^{m}\int_0^{l_k}\boldsymbol{\delta}_{kj}^{\mathrm{T}}(x)\mathbf{q}_k(x,t)\mathrm{d}x+\sum_{J=1}^{n}\left[\left(\mathbf{u}_j^J\right)^{\mathrm{T}}\mathbf{p}^J(t)\right] \tag{53}$$

A particular solution of Eq. (53) is given by the convolution integral or Duhamel integral [1] as

$$r_j(t)=\frac{1}{M_j\omega_j}\int_0^t Q_j(\tau)\sin\,\omega_j(t-\tau)\,\mathrm{d}\tau \tag{54}$$

where

$$Q_j(\tau)=\sum_{k=1}^{m}\int_0^{l_k}\boldsymbol{\delta}_{kj}^{\mathrm{T}}(x)\mathbf{q}_k(x,\tau)\,\mathrm{d}x+\sum_{J=1}^{n}\left[\left(\mathbf{u}_j^J\right)^{\mathrm{T}}\mathbf{p}^J(\tau)\right] \tag{55}$$

The complementary solution of Eq. (53) vanishes for problems with zero initial conditions. Thus, the complete solution of the forced vibration is given as the summation of the modal solutions:

$$\boldsymbol{\delta}_k(x,t)=\sum_{j=1}^{\infty}\left[\frac{1}{M_j\omega_j}\int_0^t Q_j(\tau)\sin\,\omega_j(t-\tau)\mathrm{d}\tau\right]\boldsymbol{\delta}_{kj}(x) \tag{56}$$

Other physical variables including strain, stress, generalized force, velocity, and acceleration, can be determined accordingly.

Table 1
Parameters of the 3D frame

Material parameters	Young's modulus E (Pa)	Shear modulus G (Pa)	Shear coefficient κ_z	Shear coefficient κ_y	Mass density ρ (kg/m^3)
	2.0×10^{11}	7.6923×10^{10}	$\pi^2/12$	$\pi^2/12$	7800
Geometric parameters	Area of cross-section A (m^2)	Moment of inertia I_x (m^4)	Moment of inertia I_y (m^4)	Moment of inertia I_z (m^4)	Length of structural members (m)
	0.05×0.05	1.4166×10^{-6}	5.2083×10^{-7}	5.2083×10^{-7}	$l^{12}=l^{23}=l^{35}=l^{56}=2.0$ $l^{34}=3.0$

Table 2
Natural frequencies (rad/s) of the 3D frame

Mode no.	FEM200	MRRM	Mode no.	FEM200	MRRM	Mode no.	FEM200	MRRM
1	10.51	10.51	12	324.09	324.09	35	1831.30	1831.17
2	10.89	10.89	14	388.89	388.89	40	2246.30	2248.68
3	51.89	51.89	16	463.08	463.08	45	2855.96	2855.94
4	54.68	54.68	18	735.07	735.07	50	3233.45	3235.86
5	142.94	142.94	20	800.16	800.18	55	3525.37	3526.16
6	146.84	146.84	22	872.61	872.61	60	4437.63	4437.50
7	190.87	190.87	24	974.58	974.56	70	5817.79	5817.72
8	205.22	205.22	26	1077.13	1077.13	80	6975.59	6975.72
9	244.64	244.64	28	1217.93	1217.91	90	8573.41	8572.99
10	253.32	253.32	30	1481.26	1481.29	100	9818.11	9817.88

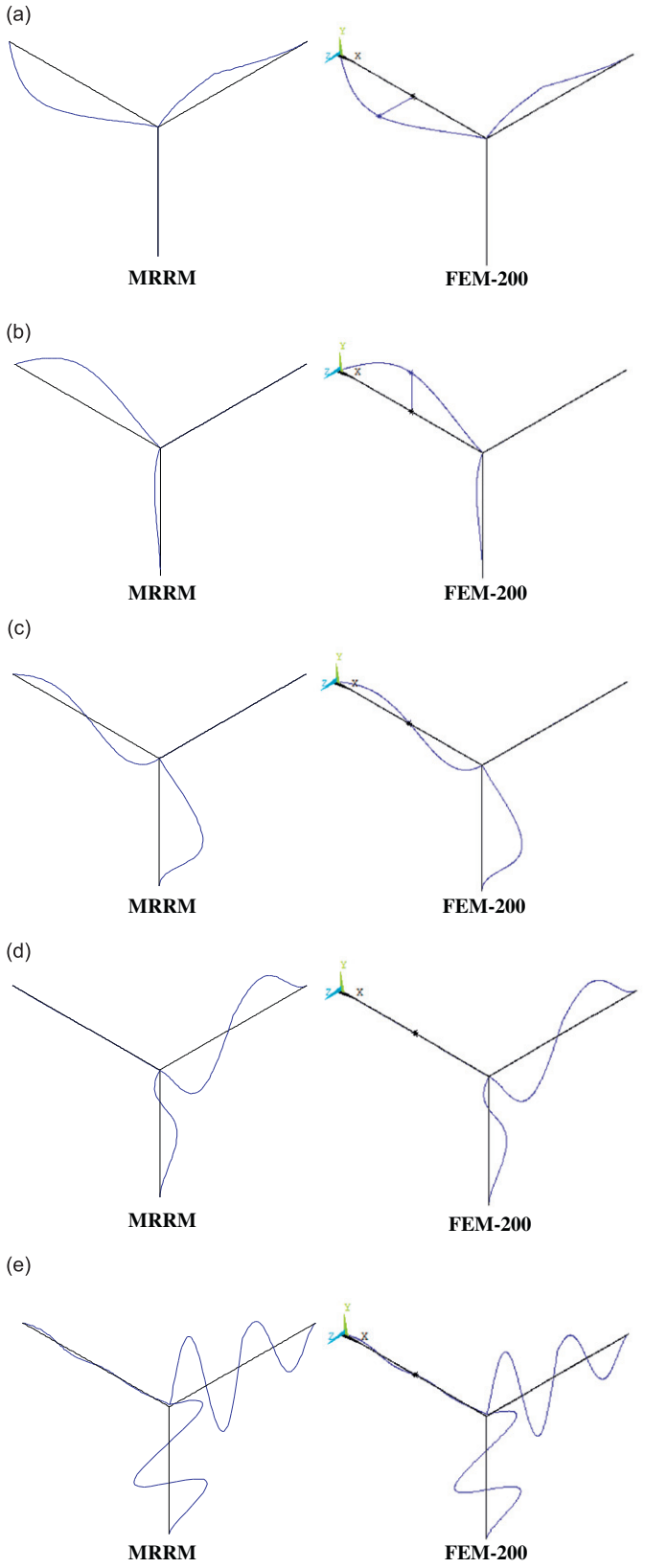

Fig. 2. Comparison of natural modes: (a) 1st mode; (b) 2nd mode; (c) 5th mode; (d) 10th mode; (e) 20th mode.

5. Numerical examples

Consider the three-dimensional frame with a lumped mass and an elastic support at joint 2 (J), as shown in Fig. 1. Note that joints K (3) and M (5) are rigid and pinned, respectively; joint I (1) is hinged, while both

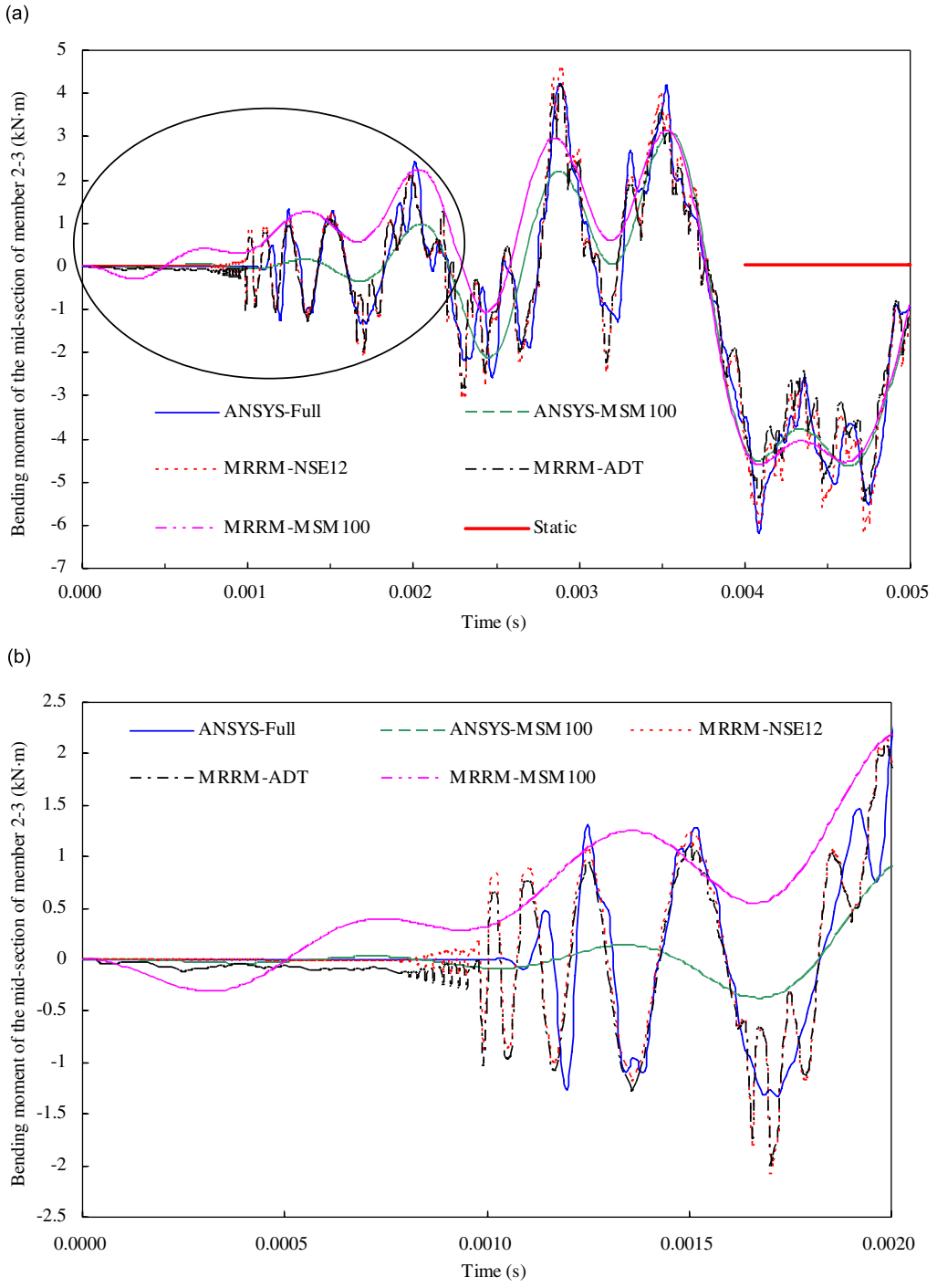

Fig. 3. Transient response of bending moment of the mid-section of member 2–3 under concentrated load at joint 5 ($t<0.005$ s): (a) response for $0\leqslant t\leqslant 0.005$ s; (b) details of response for $0\leqslant t\leqslant 0.002$.

joints L (4) and N (6) are fixed; joint J (2) is rigid, attached with a lumped mass and an elastic support. The material and geometric parameters are presented in Table 1.

The stiffness coefficient of the elastic support (along Y direction only) and the mass of the lumped body are taken as $k_y = 1000\,\mathrm{N/m}$ and $m = 1000\,\mathrm{kg}$, respectively. Dynamic analyses including free vibration and

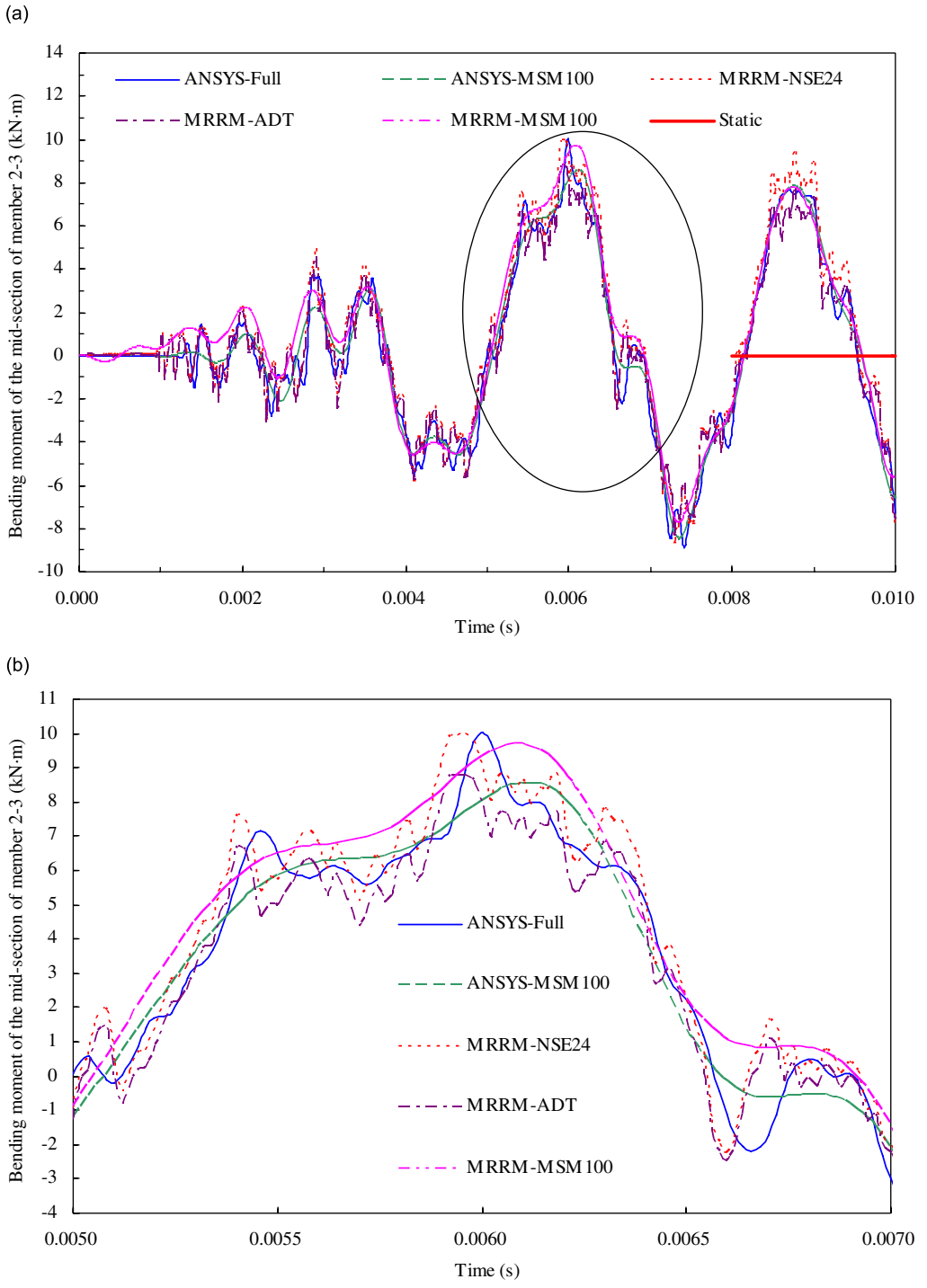

Fig. 4. Transient response of bending moment of the mid-section of member 2–3 under concentrated load at joint 5 ($t<0.01$ s): (a) response for $0\leqslant t\leqslant 0.01$ s; (b) details for $0.005\leqslant t\leqslant 0.007$ s.

transient response of the 3D frame are conducted by FEM and MRRM using various schemes. In FEM, the commercial software ANSYS is utilized and each structural member is discretized into 200 elements (the corresponding solution is indicated by FEM-200).

5.1. Free vibration

Some natural frequencies of the frame calculated by MRRM using the proposed root-searching technique outlined in Section 3.6, as well as by ANSYS, are listed in Table 2. Some natural modes calculated by MRRM according to the steps given in Section 3.6 are also compared with those calculated by ANSYS, as shown in Fig. 2. It is shown that the natural frequencies and normal modes obtained by MRRM generally agree very well with those by FEM using a very fine mesh.

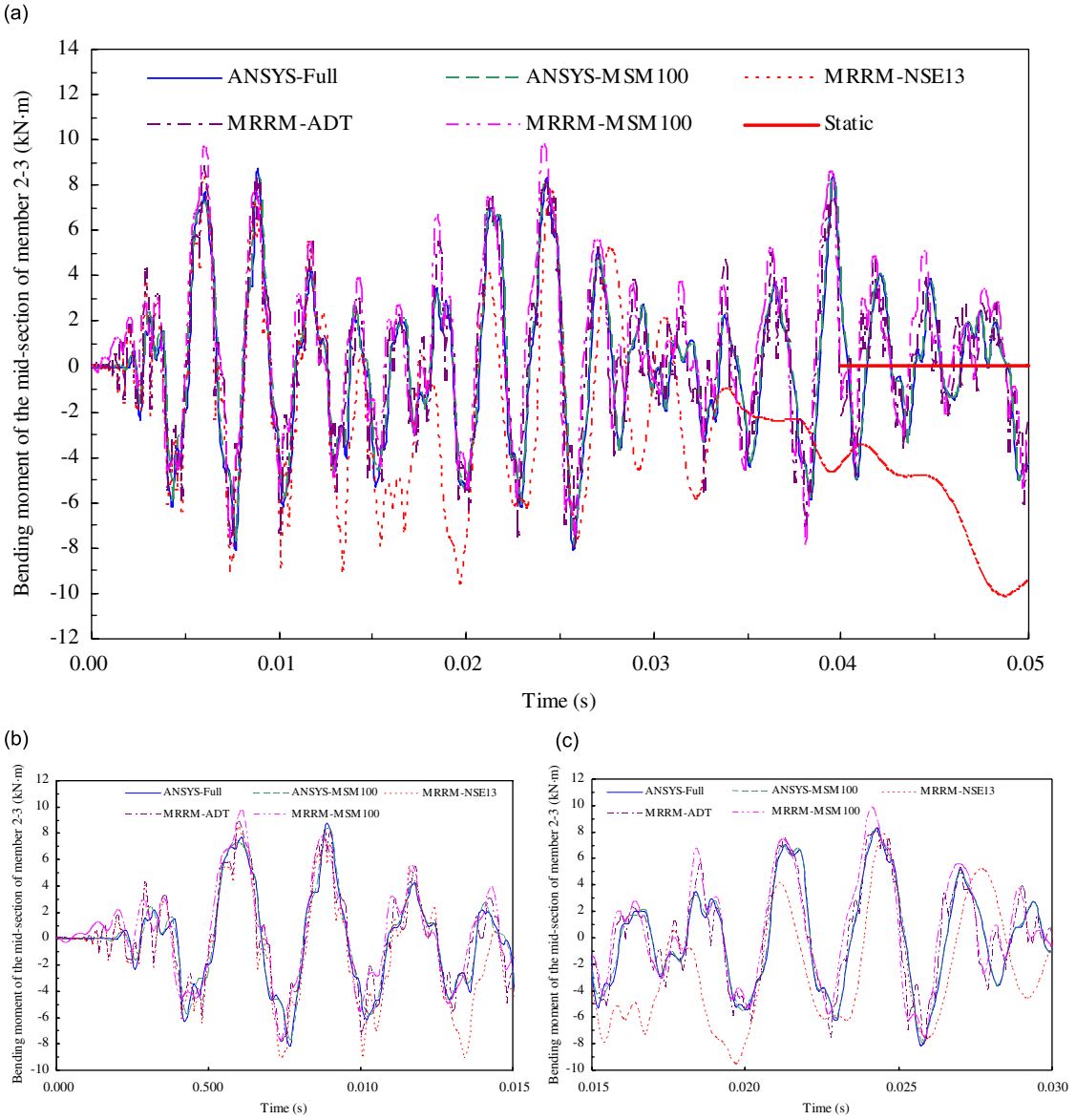

Fig. 5. Transient response of bending moment of the mid-section of member 2–3 under concentrated load at joint 5 ($t<0.05$ s): (a) response for $0\leqslant t\leqslant 0.05$ s; (b) details for $0\leqslant t\leqslant 0.015$ s; (c) details for $0.015\leqslant t\leqslant 0.030$ s.

5.2. Transient response

(1) *Response due to concentrated load applied at joint 5*: Suppose that a downward force in the form of a step function with magnitude 1000 kN is applied at joint 5 (*M*). We employ three different schemes for MRRM for comparison, including the original Neumann series expansion (MRRM-NSE) proposed in Refs. [9–13], the artificial damping technique (MRRM-ADT) suggested by Guo and Chen [14], the mode superposition method (MRRM-MSM) formulated basing on the orthogonality of natural modes put forward firstly in Ref. [35] for planar frames and extended in this paper to complex 3D frames. Furthermore, FEM analyses (ANSYS) are also performed with two different schemes, i.e. the full direct integration method (ANSYS-Full) and the mode superposition method (ANSYS-MSM100, with 100 denoting that the first 100 modes are included in the calculation). The bending moment responses at the mid-section of member 2–3 (*JK*) for periods of duration 0.005 s (Case A), 0.01 s (Case B) and 0.05 s (Case C) are calculated and are shown in Figs. 3–5. In the calculation, time steps 0.00001, 0.00002 and 0.0001 s are adopted for Cases A, B, and C, respectively. In MRRM-NSE, the first 12, 24 and 13 terms are kept in the Neumann series for Cases A, B and C, respectively, and the results are indicated by MRRM-NSEX, where $X = 12$, 24 and 13. In MRRM-ADT, the frequency independent artificial damping ratio [14] is taken to be 25.64, 12.82 and 2.564, respectively; they are determined by the rule suggested in Refs. [37,38]. Both MRRM-NSE and MRRM-ADT employ 16,384 sampling points in the inverse FFT algorithm. On the other hand, we utilize the composite trapezoidal rule (CTR) for performing the integration of the Duhamel integral in MRRM-MSM with 100 equal subintervals adopted for the integral over the length of each structural member. A total of 100 modes are taken into consideration to guarantee the convergence of calculated results.

Results in Figs. 3–5 indicate that the three methods, i.e. ANSYS-Full, ANSYS-MSM100 and MRRM-MSM100, agree with each other quite well, although difference does exist in predicting response at the very early time, for which the high-frequency components should play an important role. Note that accurate response at very early time could be obtained by MRRM-NSE [9–12] as well as MRRM-ADT [14]. Consequently, a hybrid transient analysis consisting of MRRM-NSE and MRRM-ADT for early time response and MRRM-MSM for medium-term and long-term responses shall be preferred.

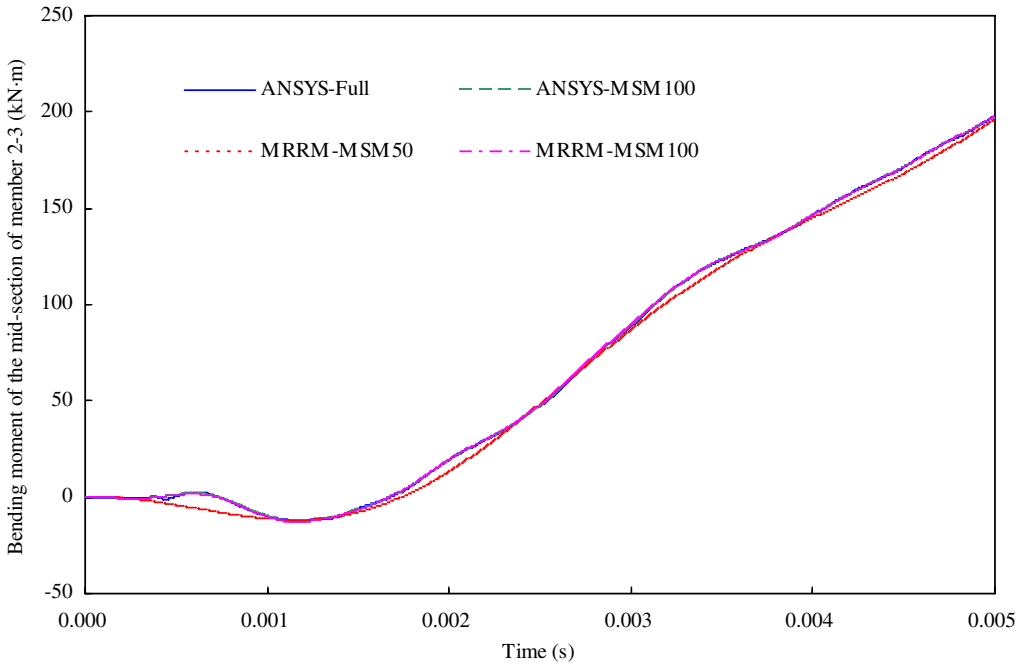

Fig. 6. Transient response of bending moment of the mid-section of member 2–3 under distributed load on member 2–3 ($t < 0.005$ s).

(2) *Response due to distributed load applied on member 2–3*: Consider a downward distributed load in the form of a step function with magnitude 1000 kN/m is uniformly applied on member 2–3 (*JK*). The bending moment responses at the mid-section of member 2–3 are calculated for periods of duration 0.005 s (Case A), 0.01 s (Case B), 0.05 s (Case C), 0.1 s (Case D) and 0.5 s (Case E). The results by the mode superposition method with MRRM for free vibration analysis (MRRM-MSM) are compared in Figs. 6–10 with those by

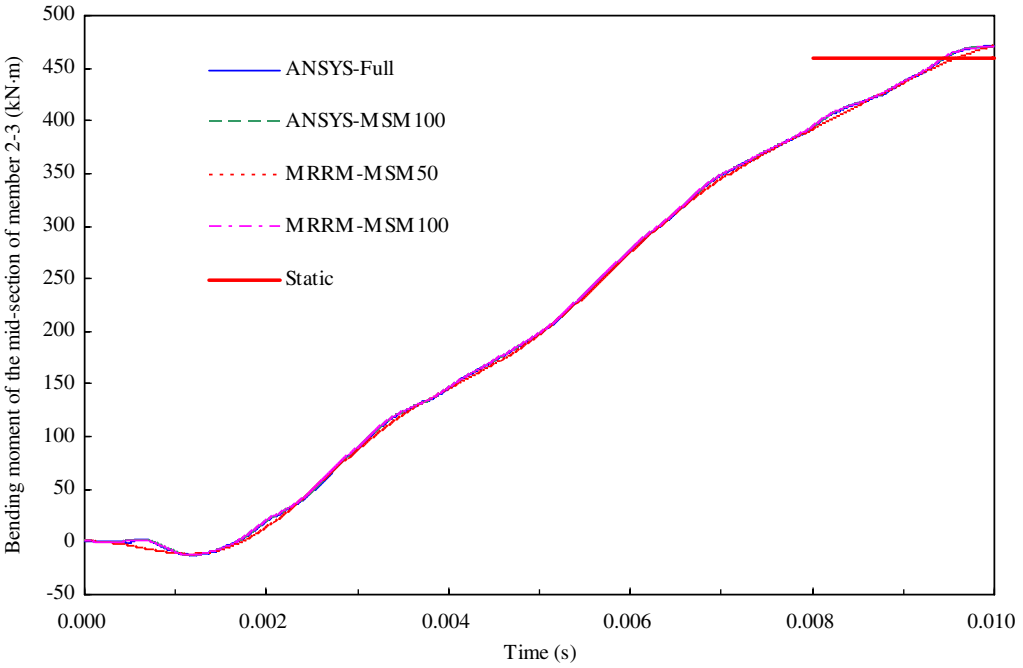

Fig. 7. Transient response of bending moment of the mid-section of member 2–3 under distributed load on member 2–3 ($t<0.01$ s).

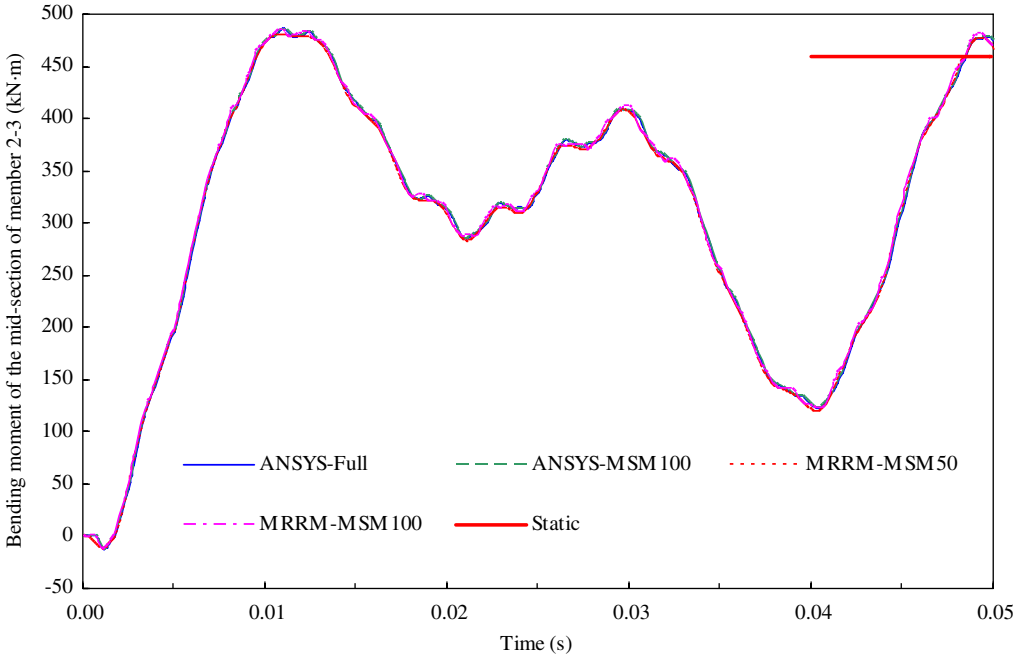

Fig. 8. Transient response of bending moment of the mid-section of member 2–3 under distributed load on member 2–3 ($t<0.05$ s).

FEM using the full direct integration scheme (ANSYS-Full) and the mode superposition scheme (ANSYS-MSM100). Different time steps 0.00001, 0.00002, 0.0001, 0.0002 and 0.001 s are adopted for Cases A–E, respectively. The same parameters as for concentrated load are used in MRRM-MSM to perform the Duhamel integral except that a number of 50 natural modes are also considered for comparison.

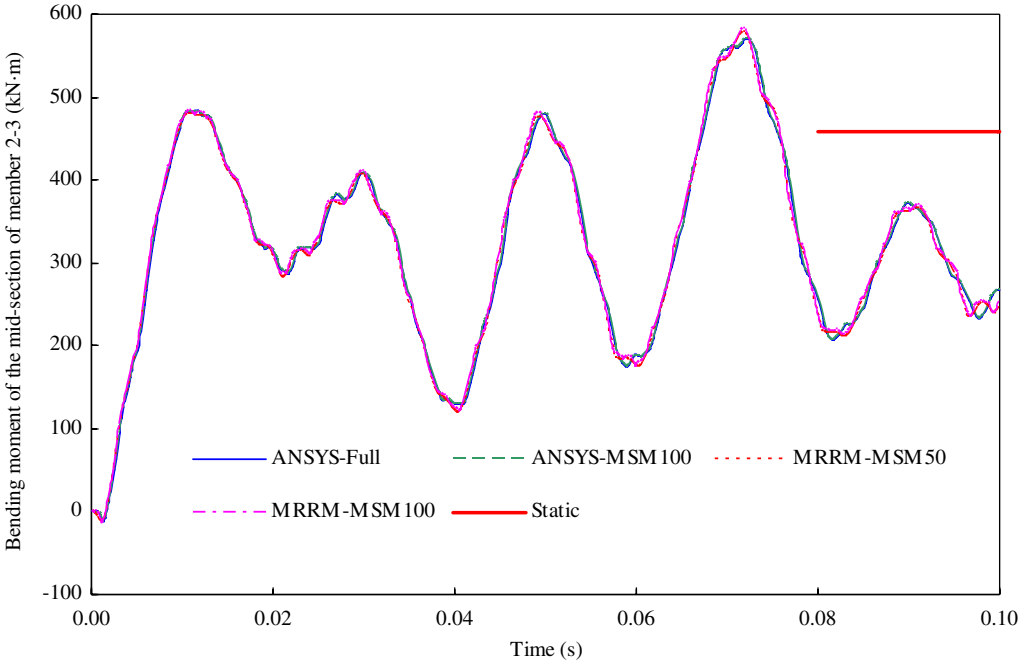

Fig. 9. Transient response of bending moment of the mid-section of member 2–3 under distributed load on member 2–3 ($t<0.1$ s).

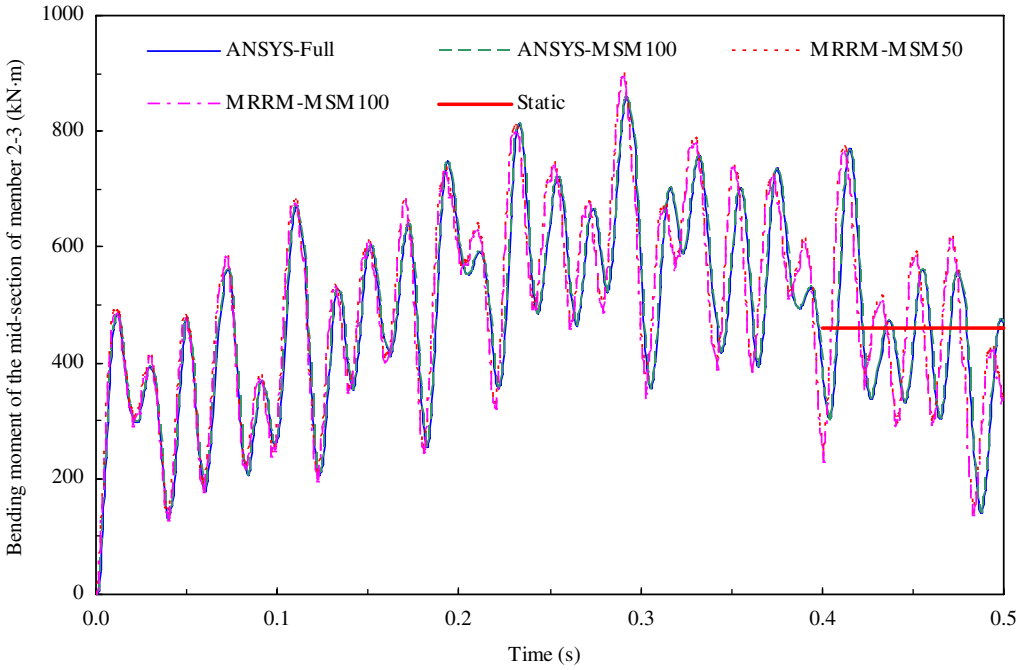

Fig. 10. Transient response of bending moment of the mid-section of member 2–3 under distributed load on member 2–3 ($t<0.5$ s).

The conclusions from the results in Figs. 6–10 are similar to those for the concentrated load case. Note that the difference between ANSYS and MRRM-MSM, although very small, increases with the time, as shown in Fig. 10. This may be due to the fact that MRRM-MSM is formulated on the continuum model, while ANSYS is based on the approximate discrete model. We also note that the results of MRRM-MSM100 and those of MRRM-MSM50 agree very well for moderate and long period of duration ($t \geqslant 0.05$ s), while small difference exists between them at early period of duration ($t < 0.05$ s). This indicates that relatively more natural modes shall be involved for response at early time when high frequency components play an important role.

6. Conclusion

The method of reverberation-ray matrix is extended to free vibration analysis of three-dimensional framed structures with optional lumped masses and/or elastic supports. Based upon Betti's reciprocity theorem, the orthogonal conditions of natural modes are established. Transient response analysis based on the expansion of normal mode is thus put forward. Such analysis is especially suitable for medium-time and long-term responses because the difficulties associated with inverse Fourier transform can be avoided. Furthermore, it can be applied for the case of distributed loads, while the original MRRM can consider concentrated loads applied at joints only.

Acknowledgements

The work was supported by the National Natural Science Foundation of China (No. 10725210 and No. 10432030), the Specialized Research Fund for the Doctoral Program of Higher Education (No. 20060335107) and the Program for New Century Excellent Talents in University (No. NCET-05-05010). The authors are very grateful to the anonymous reviewers for their constructive comments which lead to an improved version of our paper.

Appendix A. Operator matrix L

$$\mathbf{L}_{11} = \begin{bmatrix} \frac{\partial}{\partial x}\left[E(x)A(x)\frac{\partial}{\partial x}\right] & 0 & 0 \\ 0 & \frac{\partial}{\partial x}\left[\kappa_y G(x)A(x)\frac{\partial}{\partial x}\right] & 0 \\ 0 & 0 & \frac{\partial}{\partial x}\left[\kappa_z G(x)A(x)\frac{\partial}{\partial x}\right] \end{bmatrix}$$

$$\mathbf{L}_{12} = \begin{bmatrix} 0 & 0 & 0 \\ 0 & 0 & -\frac{\partial}{\partial x}[\kappa_y G(x)A(x)] \\ 0 & -\frac{\partial}{\partial x}[\kappa_z G(x)A(x)] & 0 \end{bmatrix}, \quad \mathbf{L}_{21} = \begin{bmatrix} 0 & 0 & 0 \\ 0 & 0 & \kappa_z G(x)A(x)\frac{\partial}{\partial x} \\ 0 & \kappa_y G(x)A(x)\frac{\partial}{\partial x} & 0 \end{bmatrix}$$

$$\mathbf{L}_{22} = \begin{bmatrix} \frac{\partial}{\partial x}\left[G(x)I_x(x)\frac{\partial}{\partial x}\right] & 0 & 0 \\ 0 & \frac{\partial}{\partial x}\left[E(x)I_y(x)\frac{\partial}{\partial x}\right] - \kappa_z G(x)A(x) & 0 \\ 0 & 0 & \frac{\partial}{\partial x}\left[E(x)I_z(x)\frac{\partial}{\partial x}\right] - \kappa_y G(x)A(x) \end{bmatrix}$$

Appendix B. Phase matrices

$$\mathbf{A}_\delta(x;\omega)=\begin{bmatrix} e^{ik_1x} & 0 & 0 & 0 & 0 & 0\\ 0 & e^{ik_2x} & e^{ik_3x} & 0 & 0 & 0\\ 0 & 0 & 0 & 0 & e^{ik_5x} & e^{ik_6x}\\ 0 & 0 & 0 & e^{ik_4x} & 0 & 0\\ 0 & 0 & 0 & 0 & \alpha_5e^{ik_5x} & \alpha_6e^{ik_6x}\\ 0 & \alpha_2e^{ik_2x} & \alpha_3e^{ik_3x} & 0 & 0 & 0 \end{bmatrix} \tag{B.1}$$

$$\mathbf{D}_\delta(x;\omega)=\begin{bmatrix} e^{-ik_1x} & 0 & 0 & 0 & 0 & 0\\ 0 & e^{-ik_2x} & e^{-ik_3x} & 0 & 0 & 0\\ 0 & 0 & 0 & 0 & e^{-ik_5x} & e^{-ik_6x}\\ 0 & 0 & 0 & e^{-ik_4x} & 0 & 0\\ 0 & 0 & 0 & 0 & -\alpha_5e^{-ik_5x} & -\alpha_6e^{-ik_6x}\\ 0 & -\alpha_2e^{-ik_2x} & -\alpha_3e^{-ik_3x} & 0 & 0 & 0 \end{bmatrix} \tag{B.2}$$

$$\mathbf{A}_f(x;\omega)=\begin{bmatrix} \zeta_1e^{ik_1x} & 0 & 0 & 0 & 0 & 0\\ 0 & \zeta_2e^{ik_2x} & \zeta_3e^{ik_3x} & 0 & 0 & 0\\ 0 & 0 & 0 & 0 & \zeta_5e^{ik_5x} & \zeta_6e^{ik_6x}\\ 0 & 0 & 0 & \zeta_4e^{ik_4x} & 0 & 0\\ 0 & 0 & 0 & 0 & \xi_5e^{ik_5x} & \xi_6e^{ik_6x}\\ 0 & \xi_2e^{ik_2x} & \xi_3e^{ik_3x} & 0 & 0 & 0 \end{bmatrix} \tag{B.3}$$

$$\mathbf{D}_f(x;\omega)=-\begin{bmatrix} \zeta_1e^{-ik_1x} & 0 & 0 & 0 & 0 & 0\\ 0 & \zeta_2e^{-ik_2x} & \zeta_3e^{-ik_3x} & 0 & 0 & 0\\ 0 & 0 & 0 & 0 & \zeta_5e^{-ik_5x} & \zeta_6e^{-ik_6x}\\ 0 & 0 & 0 & \zeta_4e^{-ik_4x} & 0 & 0\\ 0 & 0 & 0 & 0 & -\xi_5e^{-ik_5x} & -\xi_6e^{-ik_6x}\\ 0 & -\xi_2e^{-ik_2x} & -\xi_3e^{-ik_3x} & 0 & 0 & 0 \end{bmatrix} \tag{B.4}$$

where

$$\begin{aligned} &k_1=\omega/c_1,\quad k_{2,3}=\frac{\omega}{\sqrt{2}c_1}\sqrt{1+\frac{E}{\kappa_yG}\pm\sqrt{\left(1-\frac{E}{\kappa_yG}\right)^2+\frac{4c_1^2A}{I_z\omega^2}}},\quad k_4=\omega/c_2,\\ &k_{5,6}=\frac{\omega}{\sqrt{2}c_1}\sqrt{1+\frac{E}{\kappa_zG}\pm\sqrt{\left(1-\frac{E}{\kappa_zG}\right)^2+\frac{4c_1^2A}{I_y\omega^2}}},\quad \alpha_{2,3}=\frac{\omega^2/(\kappa_yc_2^2)-k_{2,3}^2}{ik_{2,3}},\\ &\alpha_{5,6}=\frac{\omega^2/(\kappa_zc_2^2)-k_{5,6}^2}{ik_{5,6}},\quad \zeta_1=ik_1EA,\quad \zeta_{2,3}=(ik_{2,3}-\alpha_{2,3})\kappa_yGA,\quad \zeta_4=ik_4GI_x,\\ &\zeta_{5,6}=(ik_{5,6}-\alpha_{5,6})\kappa_zGA,\quad \xi_{2,3}=ik_{2,3}\alpha_{2,3}EI_z,\quad \xi_{5,6}=ik_{5,6}\alpha_{5,6}EI_y \end{aligned} \tag{B.5}$$

References

[1] R.W. Clough, J. Penzien, *Dynamics of Structures*, second ed., McGraw-Hill, New York, 1993.
[2] F.W. Williams, W.H. Wittrick, Exact buckling and frequency calculations surveyed, *Journal of Structural Engineering ASCE* 109 (1) (1983) 169–187.

[3] F.W. Williams, Review of exact buckling and frequency calculations with optional multi-level substructuring, *Computers & Structures* 48 (3) (1993) 547–552.
[4] J.F. Doyle, *Static and Dynamic Analysis of Structures*, Kluwer Academic Publishers, Dordrecht, 1991.
[5] E.C. Pestel, F.A. Leckie, *Matrix Methods in Elastomechanics*, McGraw-Hill, New York, 1963.
[6] J.F. Doyle, *Wave Propagation in Structures*, second ed., Springer, New York, 1997.
[7] A.H. von Flotow, Disturbance propagation in structural networks, *Journal of Sound and Vibration* 106 (3) (1986) 433–450.
[8] Y. Yong, Y.K. Lin, Dynamics of complex truss-type space structures, *AIAA Journal* 28 (1990) 1250–1258.
[9] S.M. Howard, Y.H. Pao, Analysis and experiments on stress waves in planar trusses, *Journal of Engineering Mechanics ASCE* 124 (1998) 884–891.
[10] Y.H. Pao, D.C. Keh, S.M. Howard, Dynamic response and wave propagation in plane trusses and frames, *AIAA Journal* 37 (1999) 594–603.
[11] J.F. Chen, Y.H. Pao, Effects of causality and joint conditions on method of reverberation-ray matrix, *AIAA Journal* 41 (2003) 1138–1142.
[12] Y.H. Pao, G. Sun, Dynamic bending strains in planar trusses with pinned or rigid joints, *Journal of Engineering Mechanics ASCE* 129 (2003) 324–332.
[13] Y.H. Pao, W.Q. Chen, X.Y. Su, The reverberation-ray matrix and transfer matrix analyses of unidirectional wave motion, *Wave Motion* 44 (2007) 419–438.
[14] Y.Q. Guo, W.Q. Chen, Dynamic analysis of space structures with multiple tuned mass dampers, *Engineering Structures* 29 (2007) 3390–3403.
[15] K.N. Tong, *Theory of Mechanical Vibration*, Wiley, New York, 1960.
[16] S. Timoshenko, D.H. Young, W. Weaver Jr, *Vibration Problems in Engineering*, fourth ed., Wiley, New York, 1974.
[17] W.T. Thomson, *Theory of Vibration with Applications*, fourth ed., Prentice-Hall, Englewood Cliffs, New Jersey, 1993.
[18] R. Courant, D. Hilbert, *Methods of Mathematical Physics*, vol. 1, Interscience Publishers, London, 1953.
[19] E.L. Wilson, T. Itoh, An eigensolution strategy for large systems, *Computers & Structures* 16 (1983) 259–265.
[20] J.Q. Ye, F.W. Williams, Bounding properties for eigenvalues of a transcendental constrained matrix by using a simple matrix pencil, *Journal of Sound and Vibration* 177 (2) (1994) 282–287.
[21] K.L. Chan, F.W. Williams, Orthogonality of modes of structures when using the exact transcendental stiffness matrix method, *Shock and Vibration* 7 (2000) 23–28.
[22] F.W. Williams, S. Yuan, K. Ye, D. Kennedy, M.S. Djoudi, Towards deep and simple understanding of the transcendental eigenproblem of structural vibrations, *Journal of Sound and Vibration* 256 (4) (2002) 681–693.
[23] D. Kennedy, F.W. Williams, More efficient use of determinants to solve transcendental structural eigenvalue problems reliably, *Computers & Structures* 41 (5) (1991) 973–979.
[24] W.J. Watkins, D. Kennedy, F.W. Williams, Efficient parallel solution of structural eigenvalue problems, *Advances in Engineering Software* 25 (1996) 281–289.
[25] Z.H. Qi, D. Kennedy, F.W. Williams, An accurate method for transcendental eigenproblems with a new criterion for eigenfrequencies, *International Journal of Solids and Structures* 41 (2004) 3225–3242.
[26] S. Yuan, K. Ye, F.W. Williams, Second order mode-finding method in dynamic stiffness matrix methods, *Journal of Sound and Vibration* 269 (2004) 689–708.
[27] M.S. Djoudi, D. Kennedy, F.W. Williams, S. Yuan, K. Ye, Exact substructuring in recursive Newton's method for solving transcendental eigenproblems, *Journal of Sound and Vibration* 280 (2005) 883–902.
[28] Z.H. Qi, D. Kennedy, F.W. Williams, A highly stable and accurate computational method for eigensolutions in structural dynamics, *Computer Methods in Applied Mechanics and Engineering* 195 (2006) 4050–4059.
[29] Y. Tang, Numerical evaluation of uniform beam modes, *Journal of Engineering Mechanics ASCE* 129 (12) (2003) 1475–1477.
[30] R.J. Nagem, J.H. Williams, Dynamic analysis of large space structures using transfer matrices and joint coupling matrices, *Mechanics of Structures and Machines* 17 (1989) 349–371.
[31] A. Luongo, F. Romeo, Real wave vectors for dynamic analysis of periodic structures, *Journal of Sound and Vibration* 279 (2005) 309–325.
[32] J.N. Reddy, *Energy Principles and Variational Methods in Applied Mechanics*, second ed., Wiley, New York, 2002.
[33] F. Gilbert, G.E. Backus, Propagator matrices in elastic wave and vibration problems, *Geophysics* 31 (1966) 326–332.
[34] P.M. Morse, H. Feshbach, *Methods of Theoretical Physics*, McGraw Hill, New York, 1953.
[35] Y.Q. Guo, Y.H. Pao, W.Q. Chen, Orthogonality of natural modes of complex framed structures and the applications, submitted for publication.
[36] S. Barnett, *Matrices: Methods and Applications*, Oxford University Press, New York, 1990.
[37] E. Kausel, J.M. Roesset, Frequency domain analysis of undamped systems, *Journal of Engineering Mechanics ASCE* 118 (4) (1992) 721–734.
[38] J.L. Humar, H. Xia, Dynamic response analysis in frequency domain, *Earthquake Engineering and Structural Dynamics* 22 (1993) 1–12.